THE ASTROPHYSICAL JOURNAL, 468:28–50, 1996 September 1

GENERATION OF DENSITY PERTURBATIONS BY PRIMORDIAL MAGNETIC FIELDS

EUN-JIN KIM,[1] ANGELA V. OLINTO,[2] AND ROBERT ROSNER[2]
Received 1994 December 21; accepted 1996 March 7

ABSTRACT

We study the generation and evolution of density perturbations and peculiar velocities due to primordial magnetic fields. We assume that a random magnetic field was present before recombination and follow the field's effect on the baryon fluid starting at recombination. We find that magnetic fields generate growing density perturbations on length scales larger than the magnetic Jeans length, λ_B, and damped oscillations for scales smaller than λ_B. For small wavenumbers k (large length scales), we find that the magnetic field–induced density power spectrum generally scales as k^4. We derive the magnetic Jeans length explicitly by including the back-reaction of the velocity field onto the magnetic field and by decomposing the magnetic field into a force-free background field and perturbations about it. Depending on the strength of the magnetic field and the ultraviolet cutoff of its spectrum, structure can be generated on small or intermediate scales early in the history of the universe. For a present rms magnetic field of 10^{-10} G on intergalactic scales, we find that perturbations on galactic scales could have gone nonlinear at $z \simeq 6$. Finally, we discuss how primordial magnetic fields affect scenarios of structure formation with nonbaryonic dark matter.

Subject headings: cosmology: theory — galaxies: formation — large-scale structure of universe — magnetic fields — MHD

1. INTRODUCTION

The past decade has seen tremendous growth in our observational picture of the universe. The *Cosmic Background Explorer* (*COBE*) (Smoot et al. 1992) and other cosmic background experiments have shown that the large-scale clustering seen in galaxy surveys is consistent with a primordial origin for density perturbations. On the largest scales, where density perturbations are linear (i.e., rms variations in the density are smaller than the mean), microwave anisotropy observations point toward an approximately Harrison-Zeldovich spectrum of initial density perturbations [$P(k) \sim \langle|\delta_k|^2\rangle \propto k^n$, with $n \sim 1$; Smoot et al. 1992, Ganga et al. 1993]. Such a spectrum arises naturally in inflationary theories as well as in models based on topological defects.

On scales smaller than $\sim 8\,h^{-1}$ Mpc (where h is the Hubble constant in units of 100 km s^{-1} Mpc^{-1}), galaxy clustering is nonlinear, and one needs to rely on numerical studies to obtain insight into the physics of cluster and galaxy formation. (Hereafter, we set $h = 1$ unless otherwise noted.) Not only do the density perturbations become nonlinear, but the complexity of the physics involved escalates as hydrodynamical effects become important. In this paper, we show that an element of this increased complexity that is often neglected, namely magnetic fields, may play a key role in the formation of structure in the nonlinear regime.

Interest in the possibility of primordial fields has also been rekindled by recent studies of galactic dynamos, which suggest that the "classical" dynamo mechanism for galaxies, i.e., "α-ω" mean field dynamos, provide an inappropriate description of the origins of galactic magnetic fields (Ko & Parker 1989; Rosner & DeLuca 1989; Kulsrud & Anderson 1992; Chakrabarti, Rosner, & Vainshtein 1994). A variety of difficulties have been clearly recognized: To begin with, virtually all extant galactic dynamo models are kinematic, and hence they cannot properly describe the evolution of the $\beta \approx 1$ ($\beta \equiv 8\pi p/B^2$, where p is the gas pressure) galactic magnetic field. Buoyancy is typically parameterized and not explicitly taken into account (despite the fact that it is probably the dominant process by which magnetic fields generated in the solar interior and the galactic disk interior reach the outer "surfaces" of these objects; Parker 1979). The fields are assumed to be smooth; that is, there is usually no account taken of the observed filamentation and other fine structure evident in both solar magnetic fields and magnetic fields in our galaxy (although in the galactic case, it is not certain that the structure is in the field rather than in, for example, the particle density distribution). The galactic fluid is viewed as a single-component gas; this means that the effects of neutrals (including such phenomena as ambipolar diffusion) are ignored, contrary to what one would expect (in contrast, cf. Kulsrud 1988; Zweibel 1988). Finally, there is some considerable doubt as to the actual value of the turbulent (eddy) diffusivity: It has been argued by Ko & Parker (1989) that conditions appropriate to magnetic field generation and turbulent diffusion occur rather sporadically, and so they are not the norm (also Parker 1992); and various authors have argued recently that the concept of turbulent diffusion for magnetic fields is itself flawed (see Vainshtein & Rosner 1991; Kulsrud & Anderson 1992; Cattaneo & Vainshtein 1991; Cattaneo 1994; Gruzinov & Diamond 1994). Thus, although it is by no means established that dynamo models to explain galactic fields cannot be constructed (indeed, see Parker 1992 for a recent new proposal), it is by the same token no longer certain that extremely weak primordial "seed fields" are sufficient to account for the observed fields in galaxies.

Of great relevance to understanding the role of magnetic fields in galaxy formation are observations of intergalactic magnetic fields and magnetic fields at high redshifts. Reports of Faraday rotation associated with high-redshift Lyα absorp-

[1] Department of Physics and Enrico Fermi Institute, The University of Chicago, 5640 South Ellis Avenue, Chicago, IL 60637.
[2] Department of Astronomy and Astrophysics and Enrico Fermi Institute, The University of Chicago, 5640 South Ellis Avenue, Chicago, IL 60637.

tion systems (Kronberg & Perry 1982; Wolfe 1988; Wolfe, Lanzetta, & Oren 1991; Kronberg, Perry, & Zukowski 1992) suggest that dynamically significant magnetic fields may be present in condensations at high redshift. Together with observations of strong magnetic fields in clusters (Kronberg 1994), these observations support the idea that magnetic fields play a dynamical role in the evolution of structure.

The notion that magnetic fields may play an important role in structuring the universe is not new. The most detailed study was done by Wasserman (1978), who assumed the existence of a random magnetic field at recombination and, by treating it as a "source term," showed that it may act as a source for galaxy-scale density fluctuations. These calculations did not take into account the possibility of fluid back-reactions to the Lorentz force via the induction equation. Hence, the temporal evolution of the magnetic fields was due entirely to the Hubble expansion, and a magnetic Jeans length could not be derived. As we discuss below, Wasserman's approach is valid for length scales much larger than the magnetic Jeans length, λ_B, and fluid velocities much smaller than the Alfven speed, $v_A = B/(4\pi\rho)^{1/2}$. For velocities approaching v_A, the back-reaction of the fluid onto the field cannot be neglected. We study the $v \sim v_A$ regime by assuming that the background field is close to force free; this treatment allows us to derive the magnetic Jeans length within a linear analysis.

In order to describe the implications of random magnetic fields present at recombination for structure formation, we consider the coupled evolution of density perturbations, peculiar velocities, *and* magnetic fields for the following two cases. First, we study the effect of a background magnetic field to first order in the velocity and density fields (following Wasserman 1978) and deduce the spectrum of density perturbations generated on scales in which the back-reaction onto the field is small, i.e., on scales $\lambda \gg \lambda_B$. Second, we include the fluid back-reactions to the magnetic forces and consider how this type of dynamics determines the power spectrum of the resulting velocity field and density fluctuations when the background magnetic field is close to force free. Inclusion of the back-reaction onto the magnetic field allows us to derive the magnetic Jeans length for this problem, while the assumption of a force-free background field allows a linear treatment of scales $\lambda \sim \lambda_B$. Thus, we present a consistent linear perturbation analysis of the combined magnetic fluid evolution equations (in the single-fluid approximation), and we compute the present density fluctuations and vorticity under the assumption that random magnetic fields existed before recombination. We show that the resulting spectrum for density perturbations has a general form that is insensitive to the magnetic field spectral index; on large scales, the spectrum of density perturbations is too steep [$P(k) \propto k^4$] to fit the observed spectrum, while on small scales magnetic fields introduce a peak in the spectrum around $k_{\rm peak} \simeq \min(k_B, k_{\rm max})$, where $k_B = 2\pi/\lambda_B$ and $k_{\rm max}$ is the ultraviolet cutoff of the magnetic field spectrum.

The outline of our paper is as follows: We present the basic magnetohydrodynamic equations used in our analysis, discuss plausible initial conditions, and carry out our linearization in § 2. In § 3, we discuss the case studied by Wasserman and calculate the spectrum of density perturbations for this case. In § 4, we consider the case of close to force-free background magnetic fields and compute the time evolution and spectrum for the compressible modes, the resulting density fluctuations, and the incompressible modes. Our results are discussed in § 5. For the sake of clarity, we have placed details of our analysis in the Appendices.

2. THE PERTURBATION ANALYSIS

In this section, we review the physical conditions at the time of recombination, discuss the basic equations used in our analysis, and develop our perturbation scheme.

We assume that random magnetic fields were present at the epoch of recombination and that these were formed through prerecombination processes (e.g., Hogan 1983; Turner & Widrow 1988; Quashnock, Loeb, & Spergel 1989; Vaschaspati 1991; Ratra 1992a, 1992b; Cheng & Olinto 1994). As the universe cooled through recombination, baryons decoupled from the background radiation, and the baryon Jeans length decreased from scales comparable to the Hubble scale ($\sim$100 Mpc) to $\sim$10 kpc in comoving units. [Throughout this paper, we use λ to describe comoving length scales and set the scale factor today to unity, $R(t_0) \equiv 1$; physical length scales, l, at any time can be found by multiplying the comoving scale by the scale factor, $l(t) = \lambda R(t)$.] After recombination, baryons are free to condense on scales larger than the Jeans length, and they will do so via gravitational instabilities if there are initial perturbations in the density field. Concurrently, magnetic fields that were frozen into the baryon-photon plasma before recombination will tend to relax into less tangled configurations once the baryons they are coupled to decouple from the photon background. Consequently, density perturbations in the baryons can be generated through the Lorentz force even if the density field is initially smooth, and the initial peculiar velocity field vanishes at recombination. To understand the effect of magnetic fields on the origin of density perturbations, we assume that no initial density perturbations or peculiar velocities were present at recombination, so that all subsequent density perturbations or velocities are induced by magnetic fields alone. (We address the more general case of combining initial density perturbations and magnetic field effects in a subsequent paper.)

To follow the evolution of the density, peculiar velocity, and magnetic field after recombination, we write the basic one-fluid magnetohydrodynamic (MHD) equations in comoving coordinates,

$$\rho\left(\partial_t \boldsymbol{v} + \frac{\dot{R}}{R}\boldsymbol{v} + \frac{\boldsymbol{v}\cdot\nabla\boldsymbol{v}}{R}\right) = -\frac{\nabla p}{R} - \rho\frac{\nabla\psi}{R} + \frac{(\nabla\times\boldsymbol{B})\times\boldsymbol{B}}{4\pi R}, \tag{1}$$

$$\partial_t\rho + 3\frac{\dot{R}}{R}\rho + \frac{\nabla\cdot(\rho\boldsymbol{v})}{R} = 0, \tag{2}$$

$$\frac{\nabla^2\psi}{R^2} = 4\pi G[\rho - \rho_b(t)], \tag{3}$$

$$\nabla \cdot \boldsymbol{B} = 0 , \tag{4}$$

$$\partial_t(R^2\boldsymbol{B}) = \frac{\nabla \times (\boldsymbol{v} \times R^2\boldsymbol{B})}{R} \tag{5}$$

(see Wasserman 1978), where ψ is the gravitational potential, R is the scale factor, $\rho_b = \rho_b(t)$ is the uniform background density, and all other symbols have their usual meaning (we set $c = 1$ throughout the manuscript). We have neglected all viscous and diffusive terms because the relevant Reynolds numbers are very large.

2.1. *Initial Conditions and Background Evolution*

We begin with the basic assumption that all baryonic matter is distributed uniformly at recombination ($t_{\rm rec}$), with density $\rho_b(t_{\rm rec})$, and that this matter has zero peculiar velocity, $\boldsymbol{v}(\boldsymbol{x}, t_{\rm rec}) = 0$. Furthermore, we assume that there is a magnetic field already present, $\boldsymbol{B}(\boldsymbol{x}, t_{\rm rec}) = \boldsymbol{B}_{\rm rec}(\boldsymbol{x})$, presumably created well before recombination; we posit that this magnetic field is oriented randomly on spatial scales smaller than the Hubble radius at recombination *and* has no ensemble-averaged mean components on the Hubble scale; thus, we assume that $\langle \boldsymbol{B}_{\rm rec}(\boldsymbol{x}) \rangle = 0$, while $\langle |\boldsymbol{B}_{\rm rec}(\boldsymbol{x})|^2 \rangle \neq 0$, where the angle brackets mean the ensemble average.

The above magnetic field does not perturb the baryonic matter significantly until photons and baryons decouple; once decoupling occurs, the unbalanced Lorentz forces act to disturb the smooth background density, $\rho_b(t)$, leading to both density perturbations, $\delta\rho(\boldsymbol{x}, t)$, and peculiar velocities, $\boldsymbol{v}(\boldsymbol{x}, t)$, of the baryonic fluid (Wasserman 1978). We decompose the fluid density, $\rho(\boldsymbol{x}, t)$, and the magnetic field, $\boldsymbol{B}(\boldsymbol{x}, t)$, by writing

$$\rho(\boldsymbol{x}, t) = \rho_b(t) + \delta\rho(\boldsymbol{x}, t) \equiv \rho_b(t)[1 + \delta(\boldsymbol{x}, t)] ,$$

$$\boldsymbol{B}(\boldsymbol{x}, t) = \boldsymbol{B}_b(\boldsymbol{x}, t) + \delta\boldsymbol{B}(\boldsymbol{x}, t) .$$

Here $\boldsymbol{B}$ is the total field, $\boldsymbol{B}_b$ is the background random magnetic field, with

$$\boldsymbol{B}_b(\boldsymbol{x}, t) = \boldsymbol{B}_{\rm rec}(\boldsymbol{x}) \frac{R^2(t_{\rm rec})}{R^2(t)} ,$$

and $\delta\boldsymbol{B}$ is the difference between the total field and the background; in other words, $\boldsymbol{B}_b(t)$ is simply the initial random field evolved only by the Hubble flow, while $\delta\boldsymbol{B}$ is the additional field which results as the Lorentz force perturbs the baryonic fluid and the fluid reacts back.

With these definitions, we assume that at $t_{\rm rec}$,

$$\delta(\boldsymbol{x}, t_{\rm rec}) = 0 ,$$

$$\boldsymbol{v}(\boldsymbol{x}, t_{\rm rec}) = 0 ,$$

$$\delta\boldsymbol{B}(\boldsymbol{x}, t_{\rm rec}) = 0 .$$

In addition, the temporal behavior of the background quantities is determined by the cosmological model we assume. To isolate the effect of magnetic fields from other sources of density perturbation and to keep the analysis simple, we chose to study first the case of a flat universe with a critical density of baryons ($\Omega_{\rm baryon} = 1$). In § 3, § 4, and § 5, we discuss the effect on our results of including nonbaryonic dark matter as the dominant component of the universe.

For an Einstein–de Sitter model, the following relations hold during the time of interest ($0 \leq z \leq z_{\rm rec} \simeq 1100$):

$$\rho_b(t)R^3(t) = \rho_b(t_0) \equiv \rho_0 , \tag{6a}$$

$$6\pi G\rho_b(t)t^2 = 1 , \tag{6b}$$

$$R(t) = (t/t_0)^{2/3} , \tag{6c}$$

where t_0 is the age of the universe, and quantities with subscript 0 are evaluated at the present time. The background magnetic field satisfies

$$\boldsymbol{B}_b(\boldsymbol{x}, t)R^2(t) = \boldsymbol{B}_{\rm rec}(\boldsymbol{x})R^2(t_{\rm rec}) = \boldsymbol{B}_b(\boldsymbol{x}, t_0) \equiv \boldsymbol{B}_0(\boldsymbol{x}) . \tag{6d}$$

It is also useful to define

$$\langle B_0^2 \rangle \equiv \langle |\boldsymbol{B}_0(\boldsymbol{x})|^2 \rangle = 8\pi R(t)^4 \rho_B(t) , \tag{7}$$

where $\rho_B(t)$ is the average magnetic field energy density present in the universe at recombination redshifted to time t.

In analogy with the ordinary Jeans length, $\lambda_{\rm J} = v_s(\pi/\rho G)^{1/2}$, one can expect the magnetic Jeans length to be

$$\lambda_B \simeq v_{\rm A}\sqrt{\pi/\rho G}$$

(Peebles 1980). In § 4, we show that the magnetic Jeans length, defined by the wavenumber at which the transition between growing (or decaying) modes and oscillatory modes occurs, can be written as

$$\lambda_B \equiv \frac{2\pi}{k_B} = \frac{2}{5\rho_0}\sqrt{\frac{\langle B_0^2 \rangle}{G}} . \tag{8}$$

The magnetic Jeans length written above can be constrained by requiring that, at the time of nucleosynthesis, the average energy density in the magnetic field,

$$\rho_B(t) = \frac{\langle |\boldsymbol{B}(\boldsymbol{x}, t)|^2 \rangle}{8\pi} = \frac{\langle B_0^2 \rangle}{8\pi R(t)^4} ,$$

be significantly less than the energy density in radiation,

$$\rho_r(t) = \frac{\pi^2 g_* T^4}{30} ,$$

where g_* is the number of relativistic degrees of freedom, and T is the temperature of the background radiation (Barrow 1976; see also Cheng, Schramm, & Truran 1994, Grasso & Rubinstein 1995, and Kernan, Starkman, & Vachaspati 1995). Since both energy densities redshift as R^{-4}, it suffices to require that $\rho_B \ll \rho_r$ today, which gives

$$\langle B_0^2 \rangle^{1/2} \ll 4 \times 10^{-6} \text{ G} .$$

By assuming a critical density in baryons, $\rho_0 = 2 \times 10^{-29}$ g cm^{-3}, in equation (8), we can write:

$$k_B \simeq \frac{2\pi}{100 \text{ Mpc}} \left(\frac{4 \times 10^{-6} \text{ G}}{\langle B_0^2 \rangle^{1/2}} \right) . \tag{9}$$

Therefore, the constraint $\rho_B \ll \rho_r$ implies that the magnetic Jeans length today must satisfy $l_B(t_0) = \lambda_B \ll 100$ Mpc, i.e.,

$$k_B \gg \frac{2\pi}{100 \text{ Mpc}} . \tag{10}$$

(Note that if we had set $\Omega_{\text{baryon}} < 1$ in the density used in eq. [8], the effect would be to increase the maximum λ_B, thus weakening the constraint.)

It is interesting to note that, unlike the ordinary Jeans length, λ_B does not change with time; for $t_{\text{rec}} < t < t_0$, $l_B(t) = \lambda_B R(t)$.

There are several observational constraints on a primordial magnetic field, the most stringent being an upper limit on the Faraday rotation of light from distant quasars which requires that the average magnetic field on scales comparable to the present horizon, $\bar{B}_0(H_0^{-1}) \lesssim 10^{-11}$ G (Kronberg & Simard-Normandin 1976), where $H_0^{-1} \simeq 3$ Gpc. Using similar techniques to test the magnetic field on Mpc scales gives limits of $\bar{B}_0(\text{Mpc}) \lesssim 10^{-9}$ G, which is consistent with the limit one obtains by assuming that the observed galactic magnetic field is due solely to a primordial field enhanced by the collapse of the Galaxy. Expanding the volume occupied by a galactic field of $\bar{B}_{\text{gal}} \simeq 3$ μG in order to decrease the density from that in the Galaxy to the critical density gives an average field in the universe on the scale $l_g \sim$ Mpc (the comoving scale that collapsed to form a galaxy) of $\bar{B}_0(l_g) \lesssim 10^{-9}$ G (using 2×10^{-24} g cm^{-3} for the average gas density in the Galaxy, 2×10^{-29} g cm^{-3} for the average gas density in the universe, and the assumption that the field is frozen in as the gas contracts, $B \propto \rho^{2/3}$). This argument is based on the simple assumption that the magnetic field is frozen in and grows with the collapse as $B \propto \rho^{2/3}$. Kulsrud (1995) has argued that by taking into account the formation and rotation of the Galactic disk, a seed field above $\bar{B}_0(l_g) \gtrsim 10^{-12}$ G may give rise to stronger galactic fields than observed. The dynamics of the Galactic field once fields close to or even above equipartition are reached has not been understood fully yet, so we will take the limit on Mpc scale fields to be $\bar{B}_0(\text{Mpc}) \lesssim 10^{-9}$ G below.

These limits cannot be translated unambiguously into a limit on $\langle B_0^2 \rangle^{1/2}$, since $\bar{B}_0(l)$ refers to the average field on a particular scale l, for example, averaged with a window function (see eq. [42] below). This averaging procedure depends not only on the integrated power spectrum $\langle B_0^2 \rangle^{1/2}$, but on the functional form of the power spectrum $\tilde{B}^2(k)$ as well, unless $\langle B_0^2 \rangle^{1/2} \lesssim 10^{-9}$ G. We return to these constraints during our discussion of magnetic field spectra in § 3 and § 4.

2.2. *The Perturbation Scheme*

The next step is to identify our "small" quantities, which will fix the ordering of the perturbation scheme. In the spirit of a linearized theory, we shall assume that the density perturbations resulting from the Lorentz force are small, i.e., that

$$\delta \ll 1 .$$

Similarly, we assume that the induced peculiar velocities and magnetic fields are small, e.g., we assume that

$$\frac{v_{\text{rms}} \tau}{L} \ll 1 \quad \text{and} \quad \frac{|\delta \boldsymbol{B}|}{|\boldsymbol{B}_b|} \ll 1 ,$$

where τ is the characteristic timescale of the flow, v_{rms} is the rms flow speed, and L is the characteristic length scale of the flow at time $t_{\text{rec}} + \tau$. Using these scaling relationships, we linearize equations (1)–(5), noting that since we are primarily interested in wavelengths larger than the ordinary Jeans length, the pressure term may be ignored (Peebles 1980, 1993). Then, upon retaining leading order terms, we obtain

$$\partial_t \boldsymbol{v} + \frac{\dot{R}}{R} \boldsymbol{v} = -\frac{\nabla \psi}{R} + \frac{(\nabla \times \boldsymbol{B}_b) \times \boldsymbol{B}_b}{4\pi R(t) \rho_b(t)} , \tag{11}$$

$$\partial_t \delta + \frac{\nabla \cdot \boldsymbol{v}}{R} = 0 , \tag{12}$$

$$\nabla^2 \psi = 4\pi R^2 G \rho_b \delta , \tag{13}$$

$$\nabla \cdot \boldsymbol{B}_b = \nabla \cdot \delta \boldsymbol{B} = 0 , \tag{14}$$

$$\partial_t (R^2 \boldsymbol{B}_b) = 0 , \tag{15}$$

$$\partial_t (R^2 \delta \boldsymbol{B}) = \frac{\nabla \times (\boldsymbol{v} \times R^2 \boldsymbol{B}_b)}{R} . \tag{16}$$

Note that equations (15) and (16) allow us to distinguish clearly between the background field $\boldsymbol{B}_b$ and the perturbed field $\delta \boldsymbol{B}$.

The evolution of $\boldsymbol{v}$ due to the Lorentz force depends nonlinearly on $\boldsymbol{B}$. If we assume that the background field at recombination is not force free, $(\nabla \times \boldsymbol{B}_b) \times \boldsymbol{B}_b \neq 0$, the background field will generate a velocity field with $\partial_t \boldsymbol{v} \propto (\nabla \times \boldsymbol{B}_b) \times \boldsymbol{B}_b$. The fluid motion will affect the background field through equation (16), but to higher order in perturbation theory. The fluid back-reaction can be neglected to lowest order as long as $|\delta \boldsymbol{B}| \ll |\boldsymbol{B}_b|$. This is the case studied by Wasserman (1978), who derived the time evolution of density perturbations, which we review briefly in § 3.1. In § 3.2 we derive the spectrum of density perturbations for this case.

The effect of the fluid motions on the magnetic field cannot be neglected when the fluid velocities become comparable to the Alfvén speed, $v_A = B/(4\pi\rho)^{1/2}$. This can be seen by studying the effect of one k-mode of $\boldsymbol{B}_b$ in equations (11) and (16). Equation (11) gives

$$\frac{v}{v_A} \sim \frac{kt}{R} v_A ,$$

while equation (16) implies

$$\frac{\delta B}{B_b} \sim \frac{kt}{R} v_A \frac{v}{v_A} \sim \left(\frac{v}{v_A}\right)^2 .$$

Therefore, $\delta B \ll B_b$ if $v \ll v_A$, and the back-reaction of the fluid onto the field can be neglected for scales $\lambda \gg \lambda_B$.

This first-order description in which the background field is frozen in (only redshifts) is physically reasonable for scales $\lambda_B \ll \lambda \lesssim \lambda_H$, in which a tangled background field "recently" entered the horizon and had no chance to relax to a force-free configuration. For smaller scales, $\lambda \sim \lambda_B$, an alternative description is necessary. At recombination λ_H is much larger than λ_B, and for magnetic fields of interest ($\langle B_0^2 \rangle^{1/2} < 10^{-9}$ G implies $\lambda_B < 25$ kpc), scales close to λ_B have been inside the horizon for some time and will tend to relax to force-free configurations.[3] At recombination, intermediate scales ($\lambda_B \ll \lambda \ll \lambda_H$) will be relaxing toward a force-free configuration, while scales close to λ_B behave like oscillatory modes about a force-free configuration. For this range of scales, a more appropriate description of the evolution of the fluid and magnetic field can be constructed by assuming that the background field has a force-free component on intermediate to large scales, $\boldsymbol{B}_{\rm ff}$, and small-scale perturbations about this force-free configuration, $\boldsymbol{b}$,

$$\boldsymbol{B}_b = \boldsymbol{B}_{\rm ff} + \boldsymbol{b} . \tag{17}$$

By assuming that $|\boldsymbol{B}_{\rm ff}| \gg |\boldsymbol{b}|$, we can linearize equations (1) and (5) by keeping terms to first order in $\boldsymbol{v}$ and $\boldsymbol{b}$ and write

$$\partial_t \boldsymbol{v} + \frac{\dot{R}}{R} \boldsymbol{v} = -\frac{\nabla \psi}{R} + \frac{(\nabla \times \boldsymbol{B}_{\rm ff}) \times \boldsymbol{b} + (\nabla \times \boldsymbol{B}) \times \boldsymbol{B}_{\rm ff}}{4\pi R(t) \rho_b(t)} , \tag{18}$$

$$\partial_t (R^2 \boldsymbol{B}_{\rm eff}) = 0 , \tag{19}$$

$$\partial_t (R^2 \boldsymbol{b}) = \frac{\nabla \times (\boldsymbol{v} \times R^2 \boldsymbol{B}_{\rm ff})}{R} . \tag{20}$$

Equations (18)–(20) together with equations (12)–(14) allow us to study the behavior of the coupled equations when the fluid back-reaction becomes significant and the magnetic Jeans length can be derived. This approach is valid when a separation of scales between the force-free component and the perturbations about it is possible. To obtain the spectrum of the generated density perturbations in this case, we need to specify both the spectrum of $\boldsymbol{B}_{\rm ff}$ and $\boldsymbol{b}$ at recombination. Note that $[\boldsymbol{B}_b(\boldsymbol{x}, t) R^2(t)/R_{\rm rec}^2 = \boldsymbol{B}_{\rm ff}(\boldsymbol{x}, t_{\rm rec}) + \boldsymbol{b}(\boldsymbol{x}, t_{\rm rec})$ and $\delta \boldsymbol{B}(\boldsymbol{x}, t) = \boldsymbol{b}(\boldsymbol{x}, t) - \boldsymbol{b}(\boldsymbol{x}, t_{\rm rec})]$. Following this scheme, we deduce the time evolution and find λ_B in § 4.1, and we discuss the spectrum of the generated density perturbations in § 4.2.

The physical picture and plan of this paper is as follows: Starting at recombination, we follow the effect of a random magnetic field present at recombination on the velocity and density fields. For scales $\lambda_B \ll \lambda \lesssim \lambda_H$, we use the linear approach developed by Wasserman, who derived the time evolution of these fields. We recapitulate Wasserman's results in § 3.1 and

[3] There is a substantial literature on the subject of how a magnetized plasma might relax in the presence of constraints, starting with the classic papers of Woltjer (1958) and Taylor (1974). For low-β plasmas, Taylor argued that relaxation occurs such that the total helicity, $H \equiv \int d^3 \boldsymbol{A} \cdot \boldsymbol{B}$ (with the vector potential corresponding to the magnetic field $\boldsymbol{B}$) is constant; in that case, such a system will relax to its lowest energy state consistent with this fixed value of H, with the important property that the magnetic field is force free, i.e., $\nabla \times \boldsymbol{B} = \lambda(\phi) \boldsymbol{B}$, where ϕ is the flux function corresponding to $\boldsymbol{B}$. Thus, as long as one can ignore the dynamical effects of the baryons, one would expect the fields to relax to a force-free state.

derive in § 3.2 the spectrum of generated density perturbations by assuming either a power-law of a delta function spectrum for the magnetic field. We show that the power spectrum of density perturbations is too steep to fit the observed clustering of galaxies on large scales. For $\lambda \sim \lambda_B$, we derive in § 4 the time evolution and spectra for density and velocity fields by assuming a force-free background field and either a power-law or delta function spectrum for the magnetic field perturbations about the force-free background.

3. FIXED BACKGROUND MAGNETIC FIELD

In this section, we discuss first the time evolution of the compressible modes for the case in which the field has not relaxed to a force-free background configuration and acts as a fixed comoving source of density perturbations that only redshifts in time. This approach is valid to first order in perturbation theory and for scales $\lambda \gg \lambda_B$. Then we solve for the spectrum of generated velocity field and density perturbations and discuss the implications.

3.1. *Time Evolution*

When the back-reaction of the fluid onto the background magnetic field may be neglected (i.e., for $\lambda \gg \lambda_B$), we can solve for the time evolution of $\delta(\boldsymbol{x}, t)$ by taking the divergence of equation (11) and using equations (12) and (13) (Wasserman 1978). This gives

$$\partial_{tt}\delta + 2\frac{\dot{R}}{R}\partial_t\delta - 4\pi G\rho_b\delta = \frac{\nabla\cdot[(\nabla\times\boldsymbol{B}_b)\times\boldsymbol{B}_b]}{4\pi\rho_b R^2}. \tag{21}$$

Making use of the time dependence of R, ρ_b, and $\boldsymbol{B}_b$, through equation (6), we can write

$$\partial_{tt}\delta + \frac{4}{3t}\partial_t\delta - \frac{2}{3t^2}\delta = \left(\frac{t_0}{t}\right)^2\frac{\nabla\cdot[(\nabla\times\boldsymbol{B}_0)\times\boldsymbol{B}_0]}{4\pi\rho_0}. \tag{22}$$

[Note that in our convention $\rho_0 \equiv \rho_b(t_0)$, while Wasserman uses $\rho_0(t)$ for the background density.]

The time evolution of δ is then given by

$$\delta(\boldsymbol{x}, t) = t_0^2\frac{\nabla\cdot[(\nabla\times\boldsymbol{B}_0)\times\boldsymbol{B}_0]}{4\pi\rho_0}\left[\frac{9}{10}\left(\frac{t}{t_{\rm rec}}\right)^{2/3} + \frac{3}{5}\frac{t_{\rm rec}}{t} - \frac{3}{2}\right]. \tag{23}$$

The time evolution in this case is separable from the spatial dependence such that every k-mode varies the same way in time; growing modes scale as $t^{2/3}$ or as $R(t)$, while decaying modes scale as t^{-1}.

The time evolution of the compressible modes can be found via equation (8), namely,

$$\nabla\cdot\boldsymbol{v}(\boldsymbol{x}, t) = \frac{3t_{\rm rec}\nabla\cdot[(\nabla\times\boldsymbol{B}_0)\times\boldsymbol{B}_0]}{20\pi\rho_0}\left(\frac{t_0}{t_{\rm rec}}\right)^{4/3}\left[\left(\frac{t}{t_{\rm rec}}\right)^{1/3} - \left(\frac{t_{\rm rec}}{t}\right)^{4/3}\right]. \tag{24}$$

Finally, the time evolution of the incompressible modes is given by

$$\nabla\times\boldsymbol{v}(\boldsymbol{x}, t) = \frac{3t_{\rm rec}\nabla\times[(\nabla\times\boldsymbol{B}_0)\times\boldsymbol{B}_0]}{4\pi\rho_0}\left(\frac{t_0}{t_{\rm rec}}\right)^{4/3}\left[\left(\frac{t_{\rm rec}}{t}\right)^{1/3} - \left(\frac{t_{\rm rec}}{t}\right)^{2/3}\right]. \tag{25}$$

Unlike compressible modes, incompressible modes have no growing modes during the matter-dominated era.

3.2. *Spectra of Density Perturbations and Velocity Fields*

In order to obtain the spectral dependence of δ and $\boldsymbol{v}$ for a given spectrum of magnetic fields at recombination, we define the Fourier transforms of the fluid variables in comoving coordinates,

$$\delta(\boldsymbol{x}, t) = \int d^3\boldsymbol{k}\,\exp(i\boldsymbol{k}\cdot\boldsymbol{x})\tilde{\delta}(\boldsymbol{k}, t), \tag{26}$$

$$\boldsymbol{v}(\boldsymbol{x}, t) = \int d^3\boldsymbol{k}\,\exp(i\boldsymbol{k}\cdot\boldsymbol{x})\tilde{\boldsymbol{v}}(\boldsymbol{k}, t), \tag{27}$$

$$\boldsymbol{B}_0(\boldsymbol{x}) = \int d^3\boldsymbol{k}\,\exp(i\boldsymbol{k}\cdot\boldsymbol{x})\tilde{\boldsymbol{B}}(\boldsymbol{k}). \tag{28}$$

$\boldsymbol{B}_{\rm rec}(\boldsymbol{x})$ is assumed to be homogeneous and isotropic [and, obviously, so is $\boldsymbol{B}_0(\boldsymbol{x})$]; therefore, $\tilde{\boldsymbol{B}}(\boldsymbol{k})$ obeys the relation (see Kraichnan & Nagarajan 1967; Moffatt 1978)

$$\langle\tilde{B}_i(\boldsymbol{k}_1)\tilde{B}_j^*(\boldsymbol{k}_2)\rangle = \delta^3(\boldsymbol{k}_1 - \boldsymbol{k}_2)\left(\delta_{ij} - \frac{k_{1i}k_{2j}}{k_1^2}\right)\frac{\tilde{B}^2(k_1)}{2}, \tag{29}$$

where i and j label the ith and jth components of the vector $\tilde{\boldsymbol{B}}(\boldsymbol{k})$. Note that

$$\langle B_0^2\rangle \equiv 4\pi\int dk k^2\tilde{B}^2(k) = G\left(\frac{5\pi\rho_0}{k_B}\right)^2. \tag{30}$$

For the case of a fixed magnetic background field considered in this section, the spectral dependence of δ is due solely to the initial conditions at recombination. In § 4, we discuss the case in which back-reactions become important and the time dependence is a function of the wavenumber. Here it is sufficient to determine the spectral shape of $\partial_{tt}\delta$ at recombination which is given by equations (12) and (24),

$$\partial_{tt}\delta|_{t_{rec}} = -\frac{\nabla\cdot\partial_t \boldsymbol{v}(\boldsymbol{x}, t_{rec})}{R_{rec}} = \frac{\nabla\cdot[(\nabla\times\boldsymbol{B}_0)\times\boldsymbol{B}_0]}{4\pi\rho_0 R_{rec}^3}\,. \tag{31}$$

We would like to determine the spectral dependence of the ensemble average of δ by assuming a spectrum $\tilde{B}^2(k)$ for a random magnetic field at recombination as in equation (29). The ensemble average of both sides of equation (31) vanish, since there are as many positive and negative variations of $\partial_{tt}\delta$, but the relevant quantities to be computed are the ensemble averages of the square of the fluid quantities. The root mean square (rms) of the Fourier transform of the density field is defined by

$$\tilde{\delta}_{rms}(k, t) \equiv \sqrt{\langle|\tilde{\delta}(\boldsymbol{k}, t)|^2\rangle}\,.$$

Since, in the fixed background field case, the time and spectral dependencies are separable, we can write

$$\tilde{\delta}_{rms}(k, t) \equiv c(k)\tau(t)\,,$$

where

$$\tau(t) = \frac{9}{10}\left(\frac{t}{t_{rec}}\right)^{2/3} + \frac{3}{5}\frac{t_{rec}}{t} - \frac{3}{2}\,, \tag{32}$$

and $c(k)$ is determined by equation (31). The spectral dependence of $\tilde{\delta}_{rms}$ is related to the rms of the curl-free component of the velocity field, which we define by

$$\tilde{v}_{\|\,rms}(k, t) \equiv \sqrt{\langle|\tilde{v}_{\|}(\boldsymbol{k}, t)|^2\rangle}\,,$$

where $\boldsymbol{k}\cdot\tilde{\boldsymbol{v}}(\boldsymbol{k}, t) \equiv k\tilde{v}_{\|}(\boldsymbol{k}, t)$, and the subscript " $\|$ " represents the compressible (longitudinal) component of $\tilde{\boldsymbol{v}}$. Similarly, we define

$$\tilde{v}_{\perp rms}(k, t) \equiv \sqrt{\langle|\tilde{v}_{\perp}(\boldsymbol{k}, t)|^2\rangle}\,,$$

where $\boldsymbol{k}\times\tilde{\boldsymbol{v}}(\boldsymbol{k}, t) \equiv k\tilde{v}_{\perp}(\boldsymbol{k}, t)$, and the subscript " $\perp$ " represents the incompressible (transverse) component of $\tilde{\boldsymbol{v}}$.

The detailed derivation of $c(k)$ and $\tilde{v}_{\|\,rms}(k, t)$ as a function of $\tilde{B}^2(k)$ is provided in Appendix A; here we write only the solution,

$$c(k) = \frac{t_{rec}^2}{R_{rec}}\,\dot{\tilde{v}}_{\|\,rms}(k, t_{rec})k\,, \tag{33}$$

and

$$\dot{\tilde{v}}_{\|\,rms}(k, t_{rec})^2k^2 = \left(\frac{1}{4\pi\rho_0 R_{rec}^2}\right)^2\frac{V}{(4\pi)^2}\int_{k_{min}}^{k_{max}}dk_1\int_{-1}^{1}d\mu\,\frac{\tilde{B}^2(k_1)\tilde{B}^2(|\boldsymbol{k}-\boldsymbol{k}_1|)}{|\boldsymbol{k}-\boldsymbol{k}_1|^2}\,[2k^5k_1^3\mu + k^4k_1^4(1-5\mu^2) + 2k^3k_1^5\mu^3]\,, \tag{34}$$

where V is a volume factor and $\boldsymbol{k}\cdot\boldsymbol{k}_1 = kk_1\mu$.

Since a given k-mode of the velocity field is a nonlinear convolution of the magnetic field spectrum, different k-modes of $\tilde{B}(k)$ will contribute to a given mode of $\tilde{v}(k)$. In particular, if the spectrum for the magnetic field has an ultraviolet cutoff, k_{max}, the velocity field modes will be nonzero for $k \le 2k_{max}$. In principle, the lowest k-mode excited though equation (31) is $k = 0$, even if the magnetic field spectrum has an infrared cutoff, but, in practice, the Hubble radius at each time will provide an effective infrared cutoff for the density perturbations excited by the magnetic field. As we show below, the power in low k-modes is too small for the infrared cutoff to be relevant.

In what follows, we discuss two Ansätze for the functional form of the magnetic field spectrum: power laws and delta functions. The delta function Ansatz is simple to calculate and can be used to relate our results to those of Wasserman (1978) and to the more realistic case of the power-law Ansatz.

3.2.1. *Delta Function Spectra for* $\tilde{B}^2(k)$

If the magnetic field spectrum at recombination is a delta function, we can write

$$\tilde{B}^2(k) \equiv \langle B_0^2\rangle\,\frac{\delta(k-k_*)}{4\pi k^2}\,. \tag{35}$$

The initial acceleration becomes for $k \le 2k_*$,

$$\dot{\tilde{v}}_{\|\,rms}(k, t_{rec}) = \sqrt{V}\,\frac{\langle B_0^2\rangle}{(4\pi)^3\rho_0 R_{rec}^2}\,\frac{k^{1/2}}{k_*} \tag{36}$$

and zero otherwise (see Appendix A). Using equation (33) and k_B from equation (30), we find for the density spectrum

$$c(k) = \frac{25\sqrt{V}}{384\pi^2} \frac{k^{3/2}}{k_B^2 k_*} . \tag{37}$$

We can now calculate the power spectrum of density perturbations. $P(k, t)$, and the variance (rms power per logarithmic wavenumber interval), $\Delta(k, t)$, using the following definitions:

$$P(k, t) \equiv \frac{(2\pi)^3}{V} \langle |\tilde{\delta}(k, t)|^2 \rangle , \tag{38}$$

such that

$$\langle |\delta(\boldsymbol{x}, t)|^2 \rangle \equiv \int d^3\boldsymbol{k} P(k, t) ,$$

and

$$\Delta(k, t)^2 \equiv 4\pi k^3 P(k, t) = \frac{32\pi^4}{V} k^3 \langle |\tilde{\delta}(k, t)|^2 \rangle , \tag{39}$$

such that

$$\langle |\delta(\boldsymbol{x}, t)|^2 \rangle \equiv \int \Delta(k, t)^2 d \ln k .$$

For the delta function magnetic field spectrum, we obtain

$$\Delta_\delta(k, t) = \frac{25\sqrt{2}}{96} \left(\frac{k}{k_B}\right)^3 \frac{k_B}{k_*} \tau(t) . \tag{40}$$

The resulting power spectrum of magnetic field–generated density perturbations can be compared to observations of galaxy clustering, if we assume that galaxies trace the mass density distribution. The power spectrum of galaxy clustering has been measured over the range 0.1 Mpc $\lesssim 2\pi k^{-1} \lesssim 10^2$ Mpc (e.g., Geller & Huchra 1989; Efstathiou et al. 1990; Maddox et al. 1990; Collins, Nichol, & Lumsden 1992; Fisher et al. 1993), while information from anisotropies in the background radiation reaches scales comparable to the present Hubble radius $2\pi k_0^{-1} \simeq 3 \times 10^3$ Mpc (Smoot et al. 1992; Ganga et al. 1993). In the absence of bias, an estimate of the present-day scale of nonlinear clustering can be made by estimating the scale at which the rms galaxy fluctuations are unity; for optically selected galaxies, this is $l_{\rm nl}(t_0) = \lambda_{\rm nl} \simeq 8$ Mpc. On large scales ($0.01\ {\rm Mpc}^{-1} < k < k_{\rm nl}$), the observed galaxy power spectrum is consistent with a power law, $P(k) \propto k^n$, $n \simeq -1$ with a hint of a bend to larger n at the larger scales. *COBE* suggests that $P(k) \propto k$ on the largest scales. Therefore, magnetic field–induced perturbations (with a delta function magnetic field spectrum) have too steep a spectrum [$P_\delta(k) \propto k^3$] to agree with observations on large scales. As we discuss below, a similar behavior is found if $\tilde{B}^2(k)$ is a power law [in that case, $P(k) \propto k^4$]; therefore, magnetic field–induced density perturbations *cannot* reproduce the observations of structure on very large scales.

On smaller scales ($k \gtrsim 2\pi/\lambda_{\rm nl}$), magnetic field–induced perturbations may play an important role. In particular, they are of interest if $\tilde{B}(k)$ is such that $\Delta_\delta(k, t_0) \gtrsim 1$ for cosmologically relevant scales, say between clusters of galaxies ($k_{\rm cl} \simeq 2\pi/2$ Mpc) and globular clusters ($k_{\rm gl} \simeq 2\pi/10^{-2}$ Mpc). As $\Delta_\delta(k, t)$ approaches 1, the linear treatment used above breaks down. However, we can make use of our linear solution to estimate approximately the epoch, $t_{\rm nl}(k)$, at which a particular scale k becomes nonlinear by setting $\Delta[k, t_{\rm nl}(k)] \simeq 1$.

Setting $\Delta_\delta[k, t_{\rm nl}(k)] \simeq 1$, we find that $t_{\rm nl}(k)$ satisfies

$$\left[\frac{t_{\rm nl}(k)}{t_{\rm rec}}\right]^{2/3} = \frac{1 + z_{\rm rec}}{1 + z_{\rm nl}} \simeq 3 \frac{k_*}{k_B} \left(\frac{k_B}{k}\right)^3 . \tag{41}$$

The first scale to go nonlinear in this case is the smallest wavelength allowed or largest wavenumber $k = 2k_*$. The time at which perturbations with $k = 2k_*$ become nonlinear is then $t_{\rm nl}(2k_*) \simeq 1.8\ t_{\rm rec}\ (k_B/2k_*)^3$. Requiring that $t_{\rm nl}(2k_*) \leq t_0$ implies $2k_* \gtrsim 3.7 \times 10^{-2} k_B$. For example, suppose $2k_* = 0.1k_B$, which gives $t_{\rm nl}(2k_*) \simeq 1.8 \times 10^3 t_{\rm rec}$ or redshift $z_{\rm nl}(2k_*) \simeq 6$. In this case, choosing the galaxy scale to go non-linear at $z \simeq 6$, we obtain $2k_* \simeq 2\pi/{\rm Mpc}$, $k_B \simeq 2\pi/0.1$ Mpc, and the constraint equation (10) is satisfied with $\langle B_0^2 \rangle^{1/2} \simeq 4 \times 10^{-9}$ G. This scenario would correspond to the formation of galaxies around redshift 6. If, instead we choose cluster scales to go nonlinear at redshift $z_{\rm nl} = 1$, then $2k_* \simeq 2\pi/2$ Mpc and $k_B \simeq 2\pi/0.1$ Mpc, which is the same as the previous example. A final example would be to choose the nonlinear scale to be at present, $t_{\rm nl}(2k_*) = t_0$ and $2k_* = 2\pi/8$ Mpc, then $k_B = 2\pi/0.3$ Mpc, which corresponds to a field $\langle B_0^2 \rangle^{1/2} \simeq 10^{-8}$ G.

The examples given above satisfy the constraint that $\rho_B \ll \rho_\gamma$. As we mentioned before, there are other constraints on the contribution of $\tilde{B}^2(k, t)$ to a given scale in which Faraday rotation measurements can be made. Unfortunately, these measurements can only be translated to a limit on magnetic fields when assumptions about the density of ionized gas in the line of sight are made. Since we have assumed a critical density of baryons, applying the constraints from these measurements can be somewhat ambiguous in the present discussion. When we address similar effects in the presence of dark matter, some of the ambiguity will not be present (e.g., the dependence on $\Omega_{\rm baryon}$ can be kept explicitly).

Keeping in mind these limitations, we discuss briefly the implications of these constraints for the examples given above. To apply these observational constraints, we define the average field on scale l by

$$\bar{B}^2(l, t) \equiv \left\langle \left[\int d^3x \tilde{\boldsymbol{B}}(\boldsymbol{x}, t) W(\boldsymbol{x} - \boldsymbol{x}') \right]^2 \right\rangle_{x'} = \int d^3k \tilde{B}^2(k, t) |W(kl)|^2 , \tag{42}$$

where $W(\boldsymbol{x} - \boldsymbol{x}')$ is a window function that smoothes the magnetic field on scale l, and $W(kl)$ is its Fourier transform. Using a Gaussian window function $W(\boldsymbol{x} - \boldsymbol{x}') = \exp(-|\boldsymbol{x} - \boldsymbol{x}'|^2/2l^2)$ in equation (36), we find

$$\bar{B}(l, t_0) = \langle B_0^2 \rangle^{1/2} \exp\left(-\frac{k_*^2 l^2}{2} \right) .$$

Requiring that $\bar{B}(l, t_0) \leq 10^{-9}$ G for $l = l_g \simeq$ Mpc, we can write

$$k_*^2 \geq \frac{2}{l_g^2} \ln\left(\frac{2\pi}{25 \text{ kpc}} \frac{1}{k_B} \right) . \tag{43}$$

For the three examples discussed above, the formation of galaxies at $z = 6$ and the formation of clusters at $z = 1$ satisfy equation (43), while the parameters chosen for the formation of structure on scales $l_{nl}(t_0)$ today do not satisfy this constraint.

The examples discussed above demonstrate how nonlinear structures within a limited but relevant range of scales can be formed at reasonable redshifts if magnetic fields satisfying observational limits were present at recombination. Because of the steep spectrum, the scales influenced by magnetic fields are primarily in the nonlinear regime, ultimately requiring a detailed numerical study. Although the Ansatz used above for the magnetic field spectrum is not realistic, some of the results obtained above are very similar to the power-law spectrum discussed below.

Before leaving this section, we note that Wasserman (1978) discussed the case in which $\tilde{B}^2(k)$ is sharply peaked around $k = 2\pi/x_G$ (his x_G corresponds to our l_g) and wrote (his eq. [26])

$$\langle |\nabla \cdot [(\nabla \times \boldsymbol{B}_{\rm rec}) \times \boldsymbol{B}_{\rm rec}]|^2 \rangle^{1/2} \sim \left(\frac{4}{3} \right)^{1/2} \left(\frac{2\pi}{x_G} \right)^2 \langle B_{\rm rec}^2(x) \rangle ,$$

as an estimate for the effect of magnetic fields. His result corresponds to an average over the volume

$$\langle |\nabla \cdot [(\nabla \times \boldsymbol{B}_{\rm rec}) \times \boldsymbol{B}_{\rm rec}]|^2 \rangle = \frac{[4\pi\rho_b(t_{\rm rec}) R_{\rm rec}]^2}{V} \int d^3x \langle |\nabla \cdot \dot{\boldsymbol{v}}(\boldsymbol{x}, t)|^2 \rangle ,$$

which, through Parseval's theorem, can be rewritten as

$$\langle |\nabla \cdot [(\nabla \times \boldsymbol{B}_{\rm rec}) \times \boldsymbol{B}_{\rm rec}]|^2 \rangle = \frac{[4\pi\rho_b(t_{\rm rec}) R_{\rm rec}]^2}{V} (2\pi)^3 \int d^3k \langle |\boldsymbol{k} \cdot \dot{\tilde{\boldsymbol{v}}}(\boldsymbol{k}, t)|^2 \rangle .$$

Choosing $k_* = 2\pi/x_G$ in the delta function Ansatz for $\tilde{B}^2(k)$ and using equation (36), we recover Wasserman's eq. (26).

3.2.2. *Power-Law Spectra for* $\tilde{B}^2(k)$

A variety of mechanisms for generating magnetic fields before recombination have been proposed (Hogan 1983; Turner & Widrow 1988; Quashnock et al. 1989; Vaschaspati 1991; Ratra 1992a, 1992b; Dolgov & Silk 1993; Dolgov 1993; Cheng & Olinto 1994), but consensus on a well-motivated scenario is still lacking. In general, most models generate a power-law spectrum, $\tilde{B}^2(k) \propto k^q$, with a cutoff on small scales (a typical cutoff scale is some fraction of the Hubble radius when the field was generated). Of particular interest is the case of a white-noise ($q = 0$) spectrum, which would result from magnetic fields generated with similar strengths but random directions within each Hubble volume during a phase transition in the early universe (e.g., Hogan 1983). After the phase transition, this can be viewed as a random walk of field lines, with step size of the order of the coherence length (the Hubble radius at the phase transition, or some fraction of it).

The magnetic field spectrum generated in the early universe will evolve differently on different scales. On very large scales, the field is frozen into the fluid and only redshifts with the expansion of the universe, $B \propto R^{-2}$. On very small scales, the finite plasma conductivity allows diffusion of the field within the plasma. On intermediate scales, damping of the magnetohydrodynamic modes as the neutrinos decouple and later as the photons decouple will change the effective cutoff of the magnetic field spectrum to scales as large as the Silk scale (Jedamzik, Katalinic, & Olinto 1996).

Here we restrict our attention to the evolution starting at the end of recombination for a magnetic field spectrum parameterized by the power-law index q and an ultraviolet cutoff $k_{\rm max}$. We assume that, for $k_{\rm min} \leq k \leq k_{\rm max}$,

$$\tilde{B}^2(k) \equiv Ak^q , \tag{44}$$

where A is a constant, $A \simeq (q + 3)\langle B_0^2 \rangle / k_{\rm max}^{q+3}$ (for small $k_{\rm min}$). To calculate $\dot{\tilde{v}}_{\parallel \rm rms}(k, t_{\rm rec})$ analytically, we make the further assumption that the magnetic field is Gaussian distributed. The details of the algebra are left to Appendix A. To leading order in $k/k_{\rm max} \ll 1$ and for integer spectral index q between -1 and 6, we obtain the generic result that

$$\dot{\tilde{v}}_{\parallel \rm rms}(k, t_{\rm rec}) \simeq \sqrt{V} 2\epsilon_q \frac{\langle B_0^2 \rangle}{(4\pi)^3 \rho_0 R_{\rm rec}^2} \frac{k}{k_{\rm max}^{3/2}} , \tag{45}$$

where

$$\epsilon_q \equiv \frac{\sqrt{22}(q+3)}{2\sqrt{15(2q+3)}} .$$

Using equations (33) and (45), we find

$$c(k) = \frac{25\sqrt{V}}{192\pi^2}\frac{\epsilon_q k^2}{k_B^2 k_{\rm max}^{3/2}} ,$$

$$\Delta_q(k, t) \simeq \frac{25\sqrt{2}}{48}\epsilon_q\left(\frac{k}{k_B}\right)^{7/2}\left(\frac{k_B}{k_{\rm max}}\right)^{3/2}\tau(t) , \tag{46}$$

and

$$P_q(k, t) \simeq \left(\frac{25}{48}\right)^2 \frac{\epsilon_q^2}{2\pi k_{\rm max}^3}\left(\frac{k}{k_B}\right)^4 \tau(t) . \tag{47}$$

The spectrum of generated density perturbations is almost independent of the magnetic field spectral index: $\epsilon_q \simeq 1$, for $-1 \leq q \leq 6$. (This range in q spans most of the proposed primordial magnetic field spectra, with the exception of Ratra [1992a, 1992b], who proposed indices up to $q = -3$; we return to this issue in § 4.2.) In contrast, there is a strong dependence on the ultraviolet cutoff $k_{\rm max}$, which plays a role similar to k_* in the delta function Ansatz. The amplitude of the spectrum of perturbations is determined by k_B and $k_{\rm max}$. For the power-law indices discussed above, the dependence on an infrared cutoff, $k_{\rm min}$, is negligible unless $k_{\rm min}$ is larger than the wavenumber of interest.

The power spectrum is a power law, $P_q \propto k^4$, for scales inside the horizon at recombination, i.e., for $k > k_{\rm rec} = 2\pi H_{\rm rec}$, and it is steeper for $k < k_{\rm rec}$, with a cutoff at $2k_{\rm max}$. The peak power is around $k \sim 2k_{\rm max}$, although the exact behavior cannot be obtained from equation (45), since we neglected terms of higher order in $k/k_{\rm max}$.

An interesting property of the spectrum P_q is that, unlike the case of the delta function Ansatz, if we evaluate it at k_B, $P_q(k_B)$ does not depend on k_B. This implies that if we extrapolate our solution to the limit $k \sim k_B$, P_q would have a fixed shape and amplitude as k_B is changed, shifting only horizontally on a P_q versus k plot.

Before exploring the relevant ranges in $k_{\rm max}$ and k_B for the formation of structure, we discuss the observational constraints on both parameters. The constraint on k_B in equation (10) is unchanged, since it is independent of the magnetic field power spectrum, while the constraint on $k_{\rm max}$ depends on the spectral index q. For $q = 0$, the average field on scales l is given by (from eqs. [42] and [44])

$$\bar{B}(l, t_0) = \sqrt{\frac{3\sqrt{\pi}}{4}\frac{\langle B_0^2\rangle}{k_{\rm max}^3 l^3}} , \tag{48}$$

where we use the same Gaussian window function as in the previous section to smooth the field on scales l. Again, for $l \simeq l_g$, $\bar{B}(l_g, t_0) \lesssim 10^{-9}$ G, and we obtain

$$k_{\rm max} \gtrsim \frac{1}{l_g}\left(\frac{2\pi/25\ {\rm kpc}}{k_B}\right)^{2/3} , \tag{49}$$

which is more restrictive than equation (43). As q increases, the constraint becomes less severe, since the steeper the spectrum the less it contributes to $\bar{B}_l$.

We now return to the ranges in $k_{\rm max}$ and k_B that are relevant to structure formation. In an analogous way to the delta function case, small scales reach nonlinear variance ($\Delta \geq 1$) earlier than large scales, and the first scales to become nonlinear have $k \sim 2k_{\rm max}$. We define $t_{\rm nl}(k)$ again, such that $\Delta_q(k, t_{\rm nl}) = 1$, which implies:

$$\left[\frac{t_{\rm nl}(k)}{t_{\rm rec}}\right]^{2/3} \simeq \frac{1.5}{\epsilon_q}\left(\frac{k_{\rm max}}{k_B}\right)^{3/2}\left(\frac{k_B}{k}\right)^{7/2} . \tag{50}$$

Requiring that $t_{\rm nl}(k \simeq 2k_{\rm max}) \lesssim t_0$ leads to the constraint $k_{\rm max} \gtrsim 10^{-2}k_B$. This is an approximate estimate for the lower limit for $k_{\rm max}$, since equation (45) was derived in the limit of $k \ll k_{\rm max}$. If we choose again $2k_{\rm max} = 2\pi$/Mpc and require that this scale go nonlinear at redshift $z_{\rm nl} \simeq 6$, we obtain $k_B = 2\pi/11$ Mpc, which satisfies both constraints from equation (10) and equation (49). This would correspond to the formation of galaxies at redshift 6 for a background field $\langle B_0^2\rangle \simeq 4.4 \times 10^{-9}$ G and a $\bar{B}(l_g)$ just below 10^{-9} G. If, instead we require that magnetic fields form clusters of galaxies at redshift $z_{\rm nl} = 1$, that would correspond to $2k_{\rm max} = 2\pi/2$ Mpc, and it would require $k_B = 2\pi/0.12$ Mpc. This scenario satisfies equation (10) easily and may or may not satisfy equation (49), depending on the precise value for the scale at which the constraint applies and the value of the Hubble constant. (For example, if we reintroduce h-dependences, eq. [49] is satisfied for $\bar{B} \leq 10^{-9}$ G and $h = 0.5$ with $l_g \geq 1.2$ Mpc, or if $h = 0.8$ then $l_g \geq 1.7$ Mpc.) A scenario for generating structure on scales which are going nonlinear today would correspond to choosing the scale $2k_{\rm max} = 2\pi/8$ Mpc to go nonlinear at $z_{\rm nl} = 0$ which satisfies equation (10) but does not satisfy equation (49).

We see that with a more realistic choice for the power spectrum of magnetic fields at recombination, nonlinear structures in the cosmologically relevant range of scales can be formed at reasonable redshifts for field strengths that are below the present

observational limits. Some of the examples above have field strengths that are within the range of future observational capabilities (Kronberg 1994; Lee, Olinto, & Sigl 1995).

We concentrated on galaxy and cluster scales in our examples above, but another possible consequence of magnetic fields at recombination is the formation of smaller objects, such as QSOs or Population III stars, at very early times. The challenge in the formation of smaller objects is the survival of power on those scales through recombination, since photon drag damps magnetohydrodynamic modes up to the Silk mass (Jedamzik et al. 1996).

The scales on which magnetic fields generate structure are primarily in the nonlinear regime today, which limits our ability to make precise predictions within linear perturbation theory. In the case of the baryonic universe studied above, the range of scales affected by magnetic fields is quite narrow, which suggests that objects formed via magnetic field perturbations may be biased with respect to large-scale structures formed by primordial perturbations.

For completeness, we derive the spectrum of generated incompressible modes. The initial value of $\dot{\tilde{v}}_{\perp\mathrm{rms}}(k, t_{\mathrm{rec}})$ can be obtained from equation (6) by taking the curl,

$$\nabla \times \dot{\boldsymbol{v}}(\boldsymbol{x}, t_{\mathrm{rec}}) = \frac{\nabla \times [(\nabla \times \boldsymbol{B}_0) \times \boldsymbol{B}_0]}{4\pi\rho_0 R_{\mathrm{rec}}^2} .$$

Again, as in the compressible case $\langle \dot{\tilde{v}}_{\perp}(\boldsymbol{k}, t_{\mathrm{rec}}) \rangle = 0$.

If we assume a power-law Ansatz for the magnetic field spectrum, as in equation (44), we find for the incompressible velocity field spectrum

$$\dot{\tilde{v}}_{\perp\mathrm{rms}}(k, t_{\mathrm{rec}}) \simeq \frac{(q+3)\langle B_0^2 \rangle k}{(4\pi)^3 \rho_0 R_{\mathrm{rec}}^2} \sqrt{\frac{28V}{15(2q+3)k_{\mathrm{max}}^3}} .$$

Comparing to equation (45), we see that the incompressible mode is excited initially to almost the same extent as the compressible mode. Although the two modes have comparable "initial" amplitude and spectrum, they have quite different temporal evolution and remain decoupled in the linear regime.

4. FORCE-FREE BACKGROUND MAGNETIC FIELDS

In this section, we consider an alternative perturbation scheme more appropriate for scales close to λ_B. We study the effect of magnetic fields described by small-scale perturbations about a large-scale force-free background field. We derive the time evolution of the compressible and incompressible modes in § 4.1, and in § 4.2 we discuss the spectrum of the generated modes for different magnetic field spectra.

4.1. *Time Evolution*

Taking the divergence and time derivative of equation (18), and using equations (12), (13), (19), and (20), we obtain an equation for the evolution of the divergence of the velocity,

$$\partial_t [R\partial_t (R\nabla \cdot \boldsymbol{v}] - \frac{4\pi G\rho_0}{R} \nabla \cdot \boldsymbol{v} = \frac{\nabla \cdot \boldsymbol{Q}}{4\pi\rho_0 R} , \tag{51}$$

where

$$\boldsymbol{Q} \equiv [\nabla \times \nabla \times (\boldsymbol{v} \times \boldsymbol{B}_{\mathrm{ff}0})] \times \boldsymbol{B}_{\mathrm{ff}0} + (\nabla \times \boldsymbol{B}_{\mathrm{ff}0}) \times [\nabla \times (\boldsymbol{v} \times \boldsymbol{B}_{\mathrm{ff}0})] , \tag{52}$$

and $\boldsymbol{B}_{\mathrm{ff}0}$ is today's value for the force-free component of the magnetic field. Since the perturbation scheme assumes $|\boldsymbol{B}_{\mathrm{ff}0}| \gg |\boldsymbol{b}|$, $|\boldsymbol{B}_{\mathrm{ff}0}| \approx |\boldsymbol{B}_0|$. To leading order in this perturbation scheme, the time evolution is determined by $|\boldsymbol{B}_{\mathrm{ff}0}|^2$ with no contribution from $\boldsymbol{b}$, while the spectral dependence is linear in $\boldsymbol{b}$. When deriving the time evolution and the magnetic Jeans length in this section, we may use the fact that $|\boldsymbol{B}_{\mathrm{ff}0}| \approx |\boldsymbol{B}_0|$ to omit the "ff" label, but when deriving the spectrum in § 4.2, it is important to keep the distinction.

Substituting the explicit time dependence given by equations (6) and (7), we can rewrite equation (51) in the form

$$\nabla \cdot \left(\partial_{tt} \boldsymbol{v} + \frac{2}{t} \partial_t \boldsymbol{v} - \frac{4}{9t^2} \boldsymbol{v} \right) = \left(\frac{t_0}{t} \right)^2 \frac{\nabla \cdot \boldsymbol{Q}}{4\pi\rho_0} . \tag{53}$$

The evolution equation for each velocity mode $\tilde{\boldsymbol{v}}(\boldsymbol{k})$ is then obtained by inserting Fourier expressions for the velocity field (as in eq. [27]) and for the force-free background field in analogy to equation (28). Calling $\tilde{\boldsymbol{B}}_{\mathrm{ff}}(\boldsymbol{k})$ the Fourier transform of $\boldsymbol{B}_{\mathrm{ff}0}(\boldsymbol{x}, t)$ as in equation (28), we obtain

$$\boldsymbol{k} \cdot \left(t^2 \partial_{tt} + 2t\partial_t - \frac{4}{9} \right) \tilde{\boldsymbol{v}}(\boldsymbol{k}, t) = \beta \int d^3k_1 \, d^3k_2 \, F[\boldsymbol{k}, \boldsymbol{k}_1, \boldsymbol{k}_2, \tilde{\boldsymbol{B}}_{\mathrm{ff}}(\boldsymbol{k}_1), \tilde{\boldsymbol{B}}_{\mathrm{ff}}(\boldsymbol{k}_2), \tilde{\boldsymbol{v}}(\boldsymbol{k} - \boldsymbol{k}_1 - \boldsymbol{k}_2, t)] , \tag{54}$$

where

$$\beta \equiv \frac{t_0^2}{4\pi\rho_0} = \frac{1}{24\pi^2 \rho_0^2 G} ,$$

$$F \equiv -\{k^2(\tilde{\boldsymbol{B}}_1 \cdot \tilde{\boldsymbol{B}}_2)(k - k_2)_i - k^2[(\boldsymbol{k} - \boldsymbol{k}_2) \cdot \tilde{\boldsymbol{B}}_1]\tilde{B}_{2i} + 2(\boldsymbol{k} \cdot \tilde{\boldsymbol{B}}_2)[(\boldsymbol{k} \cdot \tilde{\boldsymbol{B}}_1)k_{2i} - (\boldsymbol{k}_2 \cdot \tilde{\boldsymbol{B}}_1)k_i]\}\tilde{v}_i(\boldsymbol{k} - \boldsymbol{k}_1 - \boldsymbol{k}_2, t) ,$$

$\tilde{\boldsymbol{B}}_1 \equiv \tilde{\boldsymbol{B}}_{\rm ff}(\boldsymbol{k}_1)$, and $\tilde{\boldsymbol{B}}_2 \equiv \tilde{\boldsymbol{B}}_{\rm ff}(\boldsymbol{k}_2)$. For notational convenience, we define a logarithmic time variable $T \equiv \ln t$ and define further the operator G_i such that

$$\int d^3\boldsymbol{k}_1\, d^3\boldsymbol{k}_2\, F \equiv G_i(\boldsymbol{k}:\boldsymbol{l})v_i(\boldsymbol{l}, T)\,,$$

i.e.,

$$G_i \equiv -\int d^3\boldsymbol{k}_1\, d^3\boldsymbol{k}_2\, d^3\boldsymbol{l}\{k^2(\tilde{\boldsymbol{B}}_1\cdot\tilde{\boldsymbol{B}}_2)(k-k_2)_i - k^2[(\boldsymbol{k}-\boldsymbol{k}_2)\cdot\tilde{\boldsymbol{B}}_1]\tilde{B}_{2i} + 2(\boldsymbol{k}\cdot\tilde{\boldsymbol{B}}_2)[(\boldsymbol{k}\cdot\boldsymbol{Bn}_1)k_{2i} - (\boldsymbol{k}_2\cdot\tilde{\boldsymbol{B}}_1)k_i]\}\delta(\boldsymbol{k}-\boldsymbol{k}_1-\boldsymbol{k}_2-\boldsymbol{l})\,.$$

Upon using this definition, equation (19) then reads

$$\left(\partial_{TT} + \partial_T - \frac{4}{9}\right)\tilde{v}_{\parallel}(\boldsymbol{k}, T) = \frac{\beta}{k}\, G_i(\boldsymbol{k}:\boldsymbol{l})\tilde{v}_i(\boldsymbol{l}, T)\,. \tag{55}$$

Since the ensemble average of both sides of equation (55) vanish, we compute the evolution of the quadratic quantities. At the expense of yet further algebra, one obtains the following three equations:

$$\partial_T\langle|\tilde{v}_{\parallel}(\boldsymbol{k}, T)|^2\rangle = 2\,\mathrm{Re}\,\langle\tilde{v}_{\parallel}(\boldsymbol{k}, T)\partial_T\tilde{v}^*_{\parallel}(\boldsymbol{k}, T)\rangle\,, \tag{56a}$$

$$\partial_T\,\mathrm{Re}\,\langle\tilde{v}_{\parallel}(\boldsymbol{k}, T)\partial_T\tilde{v}^*_{\parallel}(\boldsymbol{k}, T)\rangle = \frac{4}{9}\langle|\tilde{v}_{\parallel}(\boldsymbol{k}, T)|^2\rangle - \mathrm{Re}\,\langle\tilde{v}_{\parallel}(\boldsymbol{k}, T)\partial_T\tilde{v}^*_{\parallel}(\boldsymbol{k}, T)\rangle + \langle|\partial_T\tilde{v}_{\parallel}(\boldsymbol{k}, T)|^2\rangle + \frac{\beta}{k}\,\mathrm{Re}\,\langle G_i(\boldsymbol{k}:\boldsymbol{l})\tilde{v}_i(\boldsymbol{l}, T)\tilde{v}^*_{\parallel}(\boldsymbol{k}, T)\rangle\,, \tag{56b}$$

$$\partial_T\langle|\partial_T\tilde{v}_{\parallel}(\boldsymbol{k}, T)|^2\rangle = \frac{8}{9}\,\mathrm{Re}\,\langle\tilde{v}_{\parallel}(\boldsymbol{k}, T)\partial_T\tilde{v}^*_{\parallel}(\boldsymbol{k}, T)\rangle - 2\langle|\partial_T\tilde{v}_{\parallel}(\boldsymbol{k}, T)|^2\rangle + \frac{2\beta}{k}\,\mathrm{Re}\,\langle G_i(\boldsymbol{k}:\boldsymbol{l})\tilde{v}_i(\boldsymbol{l}, T)\partial_T\tilde{v}^*_{\parallel}(\boldsymbol{k}, T)\rangle\,, \tag{56c}$$

where "Re" stands for the real part. These equations look more complex than they really are because the recurring term $\langle Gvv^*\rangle$ can be calculated easily if one notes that $\langle B\tilde{v}(T)\rangle$ and $\int G\langle\tilde{v}_{\parallel}\,\tilde{v}_{\perp}\rangle$ vanish (see Appendix B). Thus,

$$\langle G_i(\boldsymbol{k}:\boldsymbol{l})\tilde{v}_i(\boldsymbol{l})\tilde{v}^*_{\parallel}(\boldsymbol{k})\rangle = -\tfrac{2}{3}\langle B^2_{\rm ff0}\rangle k^3\langle|\tilde{v}_{\parallel}(\boldsymbol{k})|^2\rangle\,,$$

and

$$\langle G_i(\boldsymbol{k}:\boldsymbol{l})\tilde{v}_i(\boldsymbol{l})\partial_T\tilde{v}^*_{\parallel}(\boldsymbol{k})\rangle = -\tfrac{2}{3}\langle B^2_{\rm ff0}\rangle k^3\langle\tilde{v}_{\parallel}(\boldsymbol{k})\partial_T\tilde{v}^*_{\parallel}(\boldsymbol{k})\rangle\,,$$

where

$$\langle B^2_{\rm ff0}\rangle \equiv 4\pi\int dk k^2\tilde{B}^2_{\rm ff}(k)\,.$$

These considerations allow us to write a single evolution equation for $\langle|\tilde{v}_{\parallel}(\boldsymbol{k}, T)|^2\rangle$,

$$\left[\partial_{TTT} + 3\partial_{TT} + \left(\frac{2}{9} + \frac{4}{3}ak^2\right)\partial_T + \left(\frac{4}{3}ak^2 - \frac{16}{9}\right)\right]\langle|\tilde{v}_{\parallel}(\boldsymbol{k}, T)|^2\rangle = 0\,, \tag{57}$$

where

$$a \equiv 2\beta\langle B^2_{\rm ff0}\rangle = \frac{\langle B^2_{\rm ff0}\rangle}{12\pi^2\rho_0^2 G}\,.$$

In addition, we have the initial conditions (at $T = T_{\rm rec}$)

$$\langle\tilde{v}_{\parallel}(\boldsymbol{k}, T = T_{\rm rec})\rangle = 0\,,$$

$$\partial_T\langle|\tilde{v}_{\parallel}(\boldsymbol{k}, T)|^2\rangle|_{T_{\rm rec}} = 2\mathrm{Re}\,\langle\tilde{v}_{\parallel}(\boldsymbol{k}, T_{\rm rec})\partial_T\tilde{v}^*_{\parallel}(\boldsymbol{k}, T_{\rm rec})\rangle = 0\,,$$

$$\partial_{TT}\langle|\tilde{v}_{\parallel}(\boldsymbol{k}, T)|^2\rangle|_{T=T_{\rm rec}} = 2\langle|\partial_T\tilde{v}_{\parallel}(\boldsymbol{k}, T_{\rm rec})|^2\rangle = 2[t_{\rm rec}\,\dot{\tilde{v}}_{\parallel\,\rm rms}(k, t_{\rm rec})]^2\,,$$

where $\dot{v} \equiv \partial_t v$ and $\tilde{v}_{\parallel\,\rm rms}(k, t) \equiv (\langle|\tilde{v}_{\parallel}(\boldsymbol{k}, t)|^2\rangle)^{1/2}$. These follow from the assumption that the velocity is zero everywhere at $t = t_{\rm rec}$. In the last initial condition above, $\dot{\tilde{v}}_{\parallel\,\rm rms}(k, t_{\rm rec})$ will be obtained later upon using equation (18).

Returning to our original time variable $t \equiv \exp(T)$, and again defining time derivatives with respect to the ordinary time t, the solution for the rms velocity can be written as follows:

1. For $k \neq k_B$,

$$\tilde{v}_{\parallel\,\rm rms}(k, t) = \dot{\tilde{v}}_{\parallel\,\rm rms}(k, t_{\rm rec})\,\frac{3t_{\rm rec}}{m}\left(\frac{t}{t_{\rm rec}}\right)^{-1/2}\left[\left(\frac{t}{t_{\rm rec}}\right)^{m/6} - \left(\frac{t}{t_{\rm rec}}\right)^{-m/6}\right]; \tag{58a}$$

2. For $k = k_B$,

$$\tilde{v}_{\|\,\mathrm{rms}}(k, t) = \dot{\tilde{v}}_{\|\,\mathrm{rms}}(k, t_{\mathrm{rec}}) t_{\mathrm{rec}} \left(\frac{t}{t_{\mathrm{rec}}}\right)^{-1/2} \ln\left(\frac{t}{t_{\mathrm{rec}}}\right), \tag{58b}$$

where $m(k) \equiv (25 - 12ak^2)^{1/2} = 5[1 - (k/k_B)^2]^{1/2}$. The transition from stable ($m^2 < 0$) to unstable ($m^2 > 0$) modes occurs at $k = k_B$, and therefore we find the magnetic Jeans length to be

$$\lambda_B \equiv \frac{2\pi}{k_B} = 2\pi \sqrt{\frac{12a}{25}} = \frac{2}{5} \frac{\langle B_{\mathrm{ff0}}^2 \rangle^{1/2}}{\rho_0 \sqrt{G}} . \tag{59}$$

Modes with length scales greater than λ_B ($k < k_B$) are unstable, while those on scales smaller than λ_B ($k > k_B$) undergo damped oscillations. As in Peebles (1980, 1993), one can roughly estimate the magnetic Jeans length by using the Alfvén speed, $v_A = B/(4\pi\rho)^{1/2}$, in place of the sound speed in the expression for the ordinary Jeans length, which gives

$$\lambda_B \sim \frac{B}{2\rho} \frac{1}{\sqrt{G}} ,$$

very close to the expression derived in equation (59).

We can now solve for

$$\tilde{\delta}_{\mathrm{rms}}(k, t) \equiv \sqrt{\langle |\tilde{\delta}(\boldsymbol{k}, t)|^2 \rangle}$$

by using the corresponding solution $\tilde{v}_{\|\,\mathrm{rms}}(k, t)$, with the initial condition

$$\tilde{\delta}_{\mathrm{rms}}(k, t_{\mathrm{rec}}) = 0 ,$$

and equation (12). The detailed derivation of $\tilde{\delta}_{\mathrm{rms}}(k, t)$ as a function of $\tilde{v}_{\mathrm{rms}}(k, t)$ is provided in Appendix C with the result

$$\frac{\partial}{\partial t} \tilde{\delta}_{\mathrm{rms}}(k, t) = k \frac{\tilde{v}_{\mathrm{rms}}(k, t)}{R(t)} .$$

Thus, we can write the solution

$$\tilde{\delta}_{\mathrm{rms}}(k, t) \equiv c(k) \tau(k, t) ,$$

where, for $k \neq k_B$,

$$\tau(k, t) = \frac{18}{m^2 - 1} \left[\left(1 + \frac{1}{m}\right) \left(\frac{t}{t_{\mathrm{rec}}}\right)^{(m-1)/6} + \left(1 - \frac{1}{m}\right) \left(\frac{t}{t_{\mathrm{rec}}}\right)^{-(m+1)/6} - 2 \right]; \tag{60a}$$

for $k = k_B$,

$$\tau(k, t) = 36 \left(\frac{t}{t_{\mathrm{rec}}}\right)^{-1/6} \left[\left(\frac{t}{t_{\mathrm{rec}}}\right)^{1/6} - 1 - \frac{1}{6} \ln\left(\frac{t}{t_{\mathrm{rec}}}\right) \right], \tag{60b}$$

and, again,

$$c(k) = \frac{t_{\mathrm{rec}}^2}{R_{\mathrm{rec}}} \dot{\tilde{v}}_{\|\,\mathrm{rms}}(k, t_{\mathrm{rec}}) k . \tag{61}$$

In the form for $\tilde{\delta}_{\mathrm{rms}}(k, t)$ defined above, $\tau(k, t)$ can be thought of as a transfer function which evolves an initial spectrum $c(k)$ from recombination to a later time t. We discuss now the behavior of $\tau(k, t)$ and leave a discussion of $c(k)$, which depends on the particular form of the magnetic field spectrum, to the next section (§ 4.2).

An interesting feature of the solution is that $\tau(k, t)$ is independent of the spectrum of the magnetic field (as long as its statistics are Gaussian) and depends only on the combinations k/k_B and t/t_{rec}. Therefore, the solution can be rescaled easily for different choices of magnetic field strength. The time evolution reduces to the usual $t^{2/3}$ growing and t^{-1} decaying modes in the limit $k/k_B \to 0$. In this limit, $m \simeq 5$, and the growth of perturbations is nearly independent of k, so that the final spectrum is mostly proportional to the initial spectrum given by $c(k)$ as in § 3. As $k \to k_B$ from below, the growth of perturbations decreases and, at $k = k_B$, the solution changes from unstable (for $k < k_B$) to damped oscillatory (for $k > k_B$).

In principle, the time evolution derived above is valid only for modes that correspond to scales smaller than the Hubble radius at recombination, $k > k_{\mathrm{rec}} \simeq 2\pi/100$ Mpc. Modes on comoving scales between the Hubble radius at recombination and the Hubble radius today have similar but delayed time evolution, since these modes start growing after they enter the Hubble radius. As we show below, the spectrum of perturbations, $c(k)$, is fairly steep for small k, so that the power for small-k modes is negligible, and we can approximate the power for $k < k_{\mathrm{rec}}$ to be zero. Alternatively, we can estimate the effect of the delayed evolution by using $t/t_{\mathrm{enter}}(k)$ instead of t/t_{rec} in $\tau(k, t)$ for modes with $k < k_{\mathrm{rec}}$, where $t_{\mathrm{enter}}(k)$ is the time a k-mode enters the Hubble radius, $t_{\mathrm{enter}}(k) = t_{\mathrm{rec}}(k_{\mathrm{rec}}/k)^3$.

In Figure 1, we plot $\tau(k, t/t_{\mathrm{rec}})$ for $k > k_{\mathrm{rec}}$ and $\tau(k, t/t_{\mathrm{enter}})$ for $k < k_{\mathrm{rec}}$ at different redshifts. (The sharp discontinuity at k_{rec} is an artifact of the approximation that recombination happened instantaneously.) We can see that, independent of the spectrum of the magnetic field, the power on scales $k \leq k_{\mathrm{rec}}$ is suppressed (by the delayed growth), as is the power on scales $k \geq k_B$. Therefore, while magnetic fields do not generate significant clustering on scales larger than $\sim 2\pi k_{\mathrm{rec}}^{-1}$ and smaller than

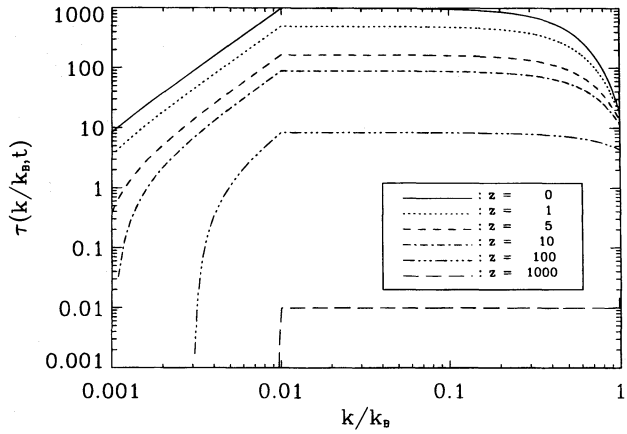

FIG. 1.—The transfer function $\tau(k, t)$ plotted vs. k/k_B for redshifts $z = 0$, 1, 5, 10, 100, and 1000. We plot $\tau(k, t/t_{rec})$ for $k > k_{rec}$ and $\tau(k, t/t_{enter})$ for $k < k_{rec}$ with $t_{enter}(k) = t_{rec}(k_{rec}/k)^3$. (We set $k_{rec} = 0.01k_B$.)

$\sim 2\pi k_B^{-1}$, they can have significant influence on the formation of structure between these two scales, depending on the strength and spectrum of magnetic fields at recombination.

If the universe were baryon dominated with infinite conductivity, magnetic fields could deter the growth of perturbations on scales smaller than λ_B; hence, a constraint on the strength of magnetic fields could be derived by the observation that structures do form on a given scale above the ordinary Jeans length λ_J. For example, for galaxies to form in a baryon-dominated, infinitely conducting flat universe, we would require $\lambda_B \lesssim l_g \simeq 1$ Mpc and, therefore, $\langle B_0^2 \rangle^{1/2} \lesssim 4 \times 10^{-8}$ G. However, this result does not take into account the presence of neutral hydrogen or nonbaryonic dark matter. When these components are present, modes on scales below λ_B are also unstable.

Finally, the time evolution of incompressible modes can be derived in an analogous manner to the derivation of the compressible mode evolution. We should note also that the incompressible modes do not affect the compressible modes just studied, and vice versa, an assertion which can be demonstrated by considering equation (20) in detail.

In order to study the incompressible modes, we take the curl and the time derivative of equation (18), use equations (19)–(20), and find

$$\nabla \times \left(\partial_{tt} \boldsymbol{v} + \frac{2}{t} \partial_t \boldsymbol{v} + \frac{2}{9t^2} \boldsymbol{v} \right) = \left(\frac{t_0}{t} \right)^2 \frac{\nabla \times \boldsymbol{Q}}{4\pi\rho_0} , \tag{62}$$

which is the incompressible analog of equation (53). Then we take Fourier transforms as in equations (27)–(28) and obtain the analog of equation (57) for the incompressible mode:

$$\left[\partial_{TTT} + 3\partial_{TT} + \left(\frac{26}{9} + \frac{2}{3} ak^2 \right) \partial_T + \left(\frac{2}{3} ak^2 + \frac{8}{9} \right) \right] \langle | \tilde{v}_\perp(\boldsymbol{k}, t)|^2 \rangle = 0 , \tag{63}$$

where $k\dot{\tilde{v}}_\perp(\boldsymbol{k}, t_{rec}) \equiv | \boldsymbol{k} \times \dot{\tilde{\boldsymbol{v}}}(\boldsymbol{k}, t_{rec}) |$.

Since the calculation is essentially the same as that described above for the compressible case, we present only the solution for the incompressible case here:

1. For $ak^2 \neq \frac{1}{6}$,

$$\tilde{v}_{\perp rms}(k, t) = \dot{\tilde{v}}_{\perp rms}(k, t_{rec}) \frac{t_{rec}}{2p} \left(\frac{t}{t_{rec}} \right)^{-1/2} \left[\left(\frac{t}{t_{rec}} \right)^p - \left(\frac{t}{t_{rec}} \right)^{-p} \right] ; \tag{64a}$$

2. For $ak^2 = \frac{1}{6}$,

$$\tilde{v}_{\perp rms}(k, t) = \dot{\tilde{v}}_{\perp rms}(k, t_{rec}) t_{rec} \left(\frac{t}{t_{rec}} \right)^{-1/2} \ln \left(\frac{t}{t_{rec}} \right) , \tag{64b}$$

where $\tilde{v}_{\perp rms}(k, t) \equiv (\langle | \tilde{v}_\perp(\boldsymbol{k}, t)|^2 \rangle)^{1/2}$, $p(k) \equiv (1 - 6ak^2)^{1/2}/6$, and $a = \langle B_{ff0}^2 \rangle / 12\pi^2 \rho_0^2 G$ is the same as in the compressible case. Unlike the compressible modes, the incompressible modes have no growing solution, only decaying or damped oscillatory solutions.

4.2. *The Spectrum of Compressible Modes*

In order to obtain the spectral dependence of the generated compressible modes, we need to find $\dot{\tilde{v}}_{\parallel rms}(k, t_{rec})$ or $c(k)$ for a given magnetic field spectrum at recombination. From equation (18),

$$\begin{aligned} \nabla \cdot \dot{\boldsymbol{v}}(\boldsymbol{x}, t_{rec}) &= \frac{\nabla \cdot \{ [(\nabla \times \boldsymbol{B}_{ffrec}) \times \boldsymbol{b}_{rec}] + [(\nabla \times \boldsymbol{b}_{rec}) \times \boldsymbol{B}_{ffrec}] \}}{4\pi\rho_b(t_{rec}) R_{rec}} \\ &= \frac{\nabla \cdot \{ [(\nabla \times \boldsymbol{B}_{ff0}) \times \boldsymbol{b}_0] + [(\nabla \times \boldsymbol{b}_0) \times \boldsymbol{B}_{ff0}] \}}{4\pi\rho_0 R_{rec}^2} , \end{aligned} \tag{65}$$

and we need to specify spectral dependencies of both $\boldsymbol{B}_{\rm ff0}$ and $\boldsymbol{b}_0$.

In what follows, we discuss two *Ansätze* for the functional form of the magnetic field spectrum. We study the solutions for the cases in which the perturbations about the force-free field are either a delta function or power laws. In both cases, we choose a delta function for the background force-free spectrum to make the problem tractable analytically. This choice describes adequately the force-free background as long as the scale of perturbations onto this background is much smaller than the background scale.

Assuming the force-free background magnetic field spectrum has a spectrum peaked at some scale, $\lambda_0 = 2\pi/k_0$, we can describe it by

$$\tilde{B}^2_{\rm ff}(k) \equiv \langle B^2_{\rm ff0}\rangle \frac{\delta(k - k_0)}{4\pi k^2} . \tag{66}$$

In Appendix D, we show that for this choice of $\tilde{B}^2_{\rm ff}(k)$ the initial acceleration can be written as

$$\langle |\boldsymbol{k}\cdot\dot{\tilde{\boldsymbol{v}}}(k, t_{\rm rec})|^2\rangle = \frac{\alpha^2\langle B^2_{\rm ff0}\rangle V}{4(4\pi)^3 k k_0^3}\int_{k_{\rm min}}^{k_{\rm max}} dk_1 \frac{\tilde{b}^2(k_1)}{k_1}\left[k_1^8 - (4k_0^2 + 2k^2)k_1^6 + (6k_0^4 + 2k^2k_0^2)k_1^4 \right.$$
$$\left. + (-4k_0^6 + 2k^2k_0^4 + 16k^4k_0^2 + 2k^6)k_1^2 + k_0^8 - 2k^2k_0^6 + 2k^6k_0^2 - k^8\right], \tag{67}$$

and $\tilde{b}^2(k_1)$ is specified in the next two sections.

4.2.1. *Delta Function Spectra for* $\tilde{b}^2(k)$

If we assume that the deviations from the force-free background are also peaked around a scale k_b, then we can write

$$\tilde{b}^2(k) \equiv \langle b_0^2\rangle \frac{\delta(k - k_b)}{4\pi k^2} , \tag{68}$$

where

$$\langle b_0^2\rangle \equiv 4\pi \int dk\, k^2 \tilde{b}^2(k) .$$

The spectrum of generated compressible modes is then given by

$$\dot{\tilde{v}}_{\parallel\,\rm rms}(k, t_{\rm rec}) = \frac{\sqrt{V\langle B^2_{\rm ff0}\rangle\langle b_0^2\rangle}}{(4\pi)^3\rho_0 R^2_{\rm rec}}\frac{2k^{1/2}}{\sqrt{k_b k_0}}\sqrt{F_\delta(k, k_0, k_b)} , \tag{69}$$

for $k_b - k_0 \le k \le k_b + k_0$, where $F_\delta(k, k_0, k_b)$ is given in Appendix D, equation (D7). Using equations (59) and (61), we find for the "initial" density spectrum

$$c(k) = \frac{25\sqrt{V}}{192\pi^2}\frac{k^{3/2}}{k_B^2\sqrt{k_b k_0}}\sqrt{\frac{\langle b_0^2\rangle}{\langle B^2_{\rm ff0}\rangle}}\,F_\delta(k, k_0, k_b) . \tag{70}$$

Although $k_b \gg k_0$ within our assumption of scale separation, we may take the limit $k_b \to k_0$ to make a connection with § 3.2.1. In this limit, we recover equation (37) with an overall factor of 2 difference due to the definitions of $\langle B^2_{\rm ff0}\rangle$, $\langle b_0^2\rangle$, and $\langle B_0^2\rangle$.

Given the linear relation between the generated compressible modes and the magnetic field perturbations about the force-free background (i.e., $\delta \propto b$), it is not surprising that the range of excited modes of δ is very narrow ($k_b - k_0 \le k \le k_b + k_0$) for the case of a delta function spectrum for b. In this scenario, only structure with $k \simeq k_b$ may form.

Although this scenario is not very realistic, we discuss briefly the formation of nonlinear structure for the following limiting cases: $k_b = k_B$ and $k_b \ll k_B$. For $k_b = k_B$, we set $\Delta(k_B, t_{\rm nl}) = c(k_B)\tau(k_B, t_{\rm nl})(32\pi^4k^3/V)^{1/2} = 1$ and find that $t_{\rm nl}$ satisfies

$$\left(\frac{t_{\rm nl}}{t_{\rm rec}}\right)^{1/6}(1 - \gamma_\delta) = 1 + \frac{1}{6}\ln\left(\frac{t_{\rm nl}}{t_{\rm rec}}\right), \tag{71}$$

where $\gamma_\delta = 3.8 \times 10^{-2}(k_0/k_B)^{1/2}(\langle B^2_{\rm ff0}\rangle/\langle b_0^2\rangle)^{1/2}$. Since $t_{\rm nl} \to t_{\rm rec}$ as $\gamma_\delta \to 0$, the smaller the k_0/k_B, the earlier nonlinear structure on scale k_B can form.

As k_b/k_B decreases from unity, the cutoff of the density spectrum becomes $k_b + k_0$ instead of k_B. For $k_b \ll k_B$, we can approximate $m \simeq 5$ in equation (60a) and write

$$\left[\frac{t_{\rm nl}(k_b)}{t_{\rm rec}}\right]^{2/3} \simeq 1.5\left(\frac{k_0}{k_b}\right)^{1/2}\left(\frac{k_B}{k_b}\right)^2\left(\frac{\langle B^2_{\rm ff0}\rangle}{\langle b_0^2\rangle}\right)^{1/2} . \tag{72}$$

The time dependence in this case is similar to the examples discussed in § 3.2.1.

The narrow range of excited modes limits the applicability of these results to physically interesting scenarios. Therefore, we move on to the more physically relevant case of power-law spectra for $\tilde{b}(k)$.

4.2.2. *Power-Law Spectra for* $\tilde{b}^2(k)$

The more general case of a power-law spectrum of magnetic field perturbations can be studied if we assume that, for $k_{\rm min} \leq k \leq k_{\rm max}$,

$$\tilde{b}^2(k) \equiv Ck^q \,, \tag{73}$$

where $C = (q+3)\,\langle b_0^2\rangle\,(k_{\rm max}^{q+3} - k_{\rm min}^{q+3})^{-1}$. For $k_{\rm min} \ll k_{\rm max}$, $C \simeq (q+3)\,\langle b_0^2\rangle\, k_{\rm max}^{-q-3}$. In Appendix D, we show that for this Ansatz (eq. (D8))

$$k^2\tilde{v}^2_{\parallel\,\rm rms}(k, t_{\rm rec}) \simeq \frac{\alpha^2 V}{4(4\pi)^4}\,\langle B^2_{\rm ff0}\rangle\langle b_0^2\rangle\,\frac{k_{\rm max}^5}{k_0^3 k}\,(q+3)F_q(k, k_0, k_{\rm max}) \,, \tag{74}$$

where $F_q(k, k_0, k_{\rm max})$ is given by equation (D9). Therefore, we find that

$$P_q(k, t) \simeq \left(\frac{25}{192}\right)^2 \frac{r(q+3)}{2\pi}\,\frac{k_{\rm max}^5}{k_B^4 k_0^3 k}\,F_q(k, k_0, k_{\rm max})\tau(k, t)^2 \,, \tag{75}$$

and

$$\Delta_q(k, t) \simeq \frac{25}{96}\sqrt{\frac{r(q+3)F_q(k, k_0, k_{\rm max})}{2}}\left(\frac{k_{\rm max}}{k_0}\right)^{3/2}\frac{k_{\rm max}\,k}{k_B^2}\,\tau(k, t) \,, \tag{76}$$

where

$$r \equiv \frac{\langle b_0^2\rangle}{\langle B^2_{\rm ff0}\rangle} \,.$$

In Figure 2, we plot $F_q(k, k_0, k_{\rm max})$ for different choices of q with fixed $k_0/k_{\rm max} = 10^{-4}$. If we take the limit $k_0/k_{\rm max} \to 0$ in equation (D5) (note that the limits of integration depend on k_0), F_q can be approximated by

$$F_q \simeq 16\left(\frac{k_0}{k_{\rm max}}\right)^3\left(\frac{k}{k_{\rm max}}\right)^{q+5} \,,$$

as is clearly shown in Figure 2. We can, therefore, write

$$P_q(k, t) \simeq \left(\frac{25}{48}\right)^2 \frac{r(q+3)}{2\pi}\,\frac{k_{\rm max}}{k_B^4}\left(\frac{k}{k_{\rm max}}\right)^{q+4}\tau(k, t)^2 \,, \tag{77}$$

and

$$\Delta_q(k, t) \simeq \frac{25}{24}\sqrt{\frac{r(q+3)}{2}}\left(\frac{k_{\rm max}}{k_B}\right)^2\left(\frac{k}{k_{\rm max}}\right)^{(q+7)/2}\tau(k, t) \,. \tag{78}$$

The spectrum of generated density perturbations in this case depends on both the magnetic field spectral index ($P_q \propto k^{q+4}$, for $k \ll k_B$) and the ultraviolet cutoff $k_{\rm max}$. The amplitude of density perturbations is determined by k_B, $k_{\rm max}$, and r, the ratio between the energy density in magnetic perturbations relative to that of the background field. We have concentrated on $q \geq -3$ such that the dependence on $k_{\rm min}$ is negligible. The results can be extended easily for cases in which $k_{\rm min}$ plays an important role.

As an example, we choose the case of $q = 0$ and plot $\Delta_0(k, t)/(r)^{1/2}$ at different redshifts in Figure 3, assuming $k_B = k_{\rm max}$, $k_0 = 10^{-4}k_{\rm max}$, and $k_{\rm min} = 10^{-3}k_{\rm max}$. For $k \ll k_{\rm max}$, $P_q \propto k^4$, and the peak power is at $k \sim k_{\rm max} = k_B$. In this example, the behavior at small k is too steep to fit large-scale structure observations, and structure will be formed primarily around the

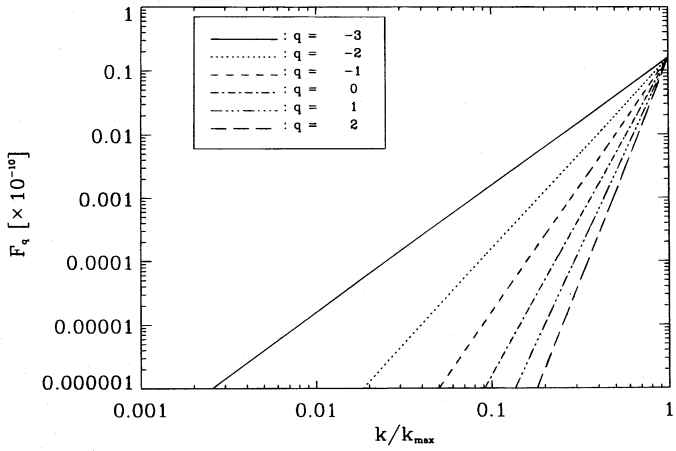

FIG. 2.—The function F_q for the power-law *Ansatz* as a function of $k/k_{\rm max}$, for $k_0 = 10^{-4}k_{\rm max}$, $k_{\rm min} = 10^{-3}k_{\rm max}$, and $q = -3, -2, -1, 0, 1, 2$

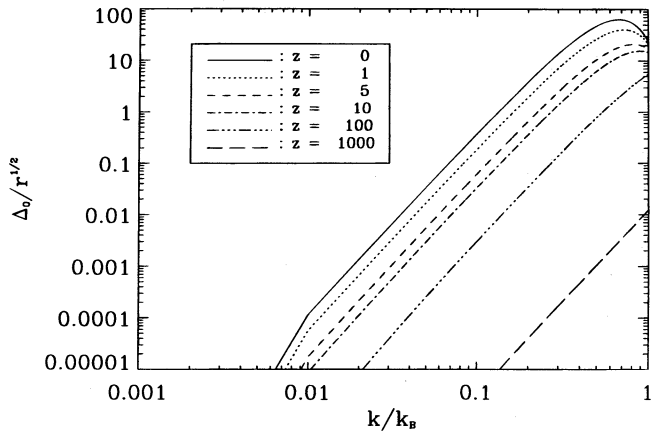

FIG. 3.—The variance for the power-law *Ansatz* with $q = 0$, $\Delta_0/(r)^{1/2}$, as a function of k/k_B for redshifts $z = 0$, 1, 5, 10, 100, and 1000. (We set $k_{max} = 10^{-3}k_{min} = 10^4 k_0$ as in Fig. 2.)

scale k_{max} or k_B. To broaden the influence of magnetic fields on the range of linear structure, a spectral index $q \sim -3$ is necessary (see Ratra 1992a, 1992b for an example of $q = -3$ primordial magnetic field spectrum.

We discuss now some examples within the large parameter space (k_{max}, k_0, k_B, and r) that are relevant to the formation of structure in the universe. As long as $q \geq -3$, the first scales to become nonlinear have $k \sim \min(k_{max}, k_B)$. We define again $t_{nl}(k)$, such that $\Delta_q(k, t_{nl}) = 1$. For $k_{max} + k_0 > k_B$, k_B is the largest mode to be excited. Setting $\Delta_q(k_B, t_{nl}) = 1$ also leads to equation (71), but with

$$\gamma_q \simeq \frac{3.8 \times 10^{-2}}{\sqrt{r(q+3)}} \left(\frac{k_{max}}{k_B}\right)^{(q+3)/2} .$$

Since as $\gamma_q \to 0$, $t_{nl} \to t_{rec}$, for $k_{max} + k_0 > k_B$ the closer k_{max} is to k_B, the earlier structures on scale k_B can form.

To simplify our discussion, we set $q = 0$ and $r = 1$ and vary k_{max}, k_B, and k_0 (different choices of q and r can be accommodated by making the appropriate rescaling of k_{max}). We find that for $k_{max} \simeq k_B$, the first nonlinear objects could form as early as redshift $z_{nl}(k_B) \simeq 300$, and the scale of nonlinearity today would be $k_{nl}(t_0) \simeq 0.15\, k_B$. If we set $k_{nl}(t_0) = 2\pi/8$ Mpc, then $k_{max} \simeq k_B \simeq 2\pi/1$ Mpc, which satisfies equation (10). Since the background field is a delta function, the appropriate bound on the parameters due to the upper limit on magnetic fields on Mpc scales is given by equation (43), with k_0 substituted for k_* (as long as $r \ll 1$). In this example, equation (43) is satisfied if $k_0 = 2\pi/2$ Mpc. If, instead, we choose $k_{nl}(t_0) = 2\pi/2$ Mpc, then $k_{max} \simeq k_B \simeq 2\pi/0.3$ Mpc, which satisfied equations (10) and (43) with $\langle B_0^2 \rangle^{1/2} \simeq 10^{-8}$ G and $\bar{B}(l_g, t_0) \simeq 10^{-10}$ G (for $k_0 \simeq 2\pi/2$ Mpc).

The time at which modes with $k = k_B$ become nonlinear, $t_{nl}(k_B)$, increases as k_{max}/k_B grows from unity. For magnetic fields to play a role in structure formation, $t_{nl}(k_B)$ must be less than the age of the universe, t_0, which implies that $k_{max} \lesssim 6k_B$.

As k_{max}/k_B decreases, so does $t_{nl}(k_B)$ up to $k_{max} + k_0 \simeq k_B$, where the cutoff changes from k_B to $k_{max} + k_0$. For $k_{max} + k_0 < k_B$, we follow $t_{nl}(k_{max})$ using our solution (eq. [60a]) in the limit $k \ll k_B$ ($m \simeq 5$), which implies

$$\left[\frac{t_{nl}(k)}{t_{rec}}\right]^{2/3} \simeq \frac{1.5}{\sqrt{r(q+3)}} \left(\frac{k_B}{k_{max}}\right)^2 \left(\frac{k_{max}}{k}\right)^{(q+7)/2} . \quad (79)$$

From equation (79), requiring $t_{nl}(k_{max}) \lesssim t_0$ leads to the constraint $k_{max} \gtrsim 10^{-2}k_B$. This estimate helps define the range for which magnetic fields can make nonlinear structures, i.e., $10^{-2}k_B \lesssim k_{max} \lesssim 6k_B$. For example, we can choose $k_{max} \simeq 0.1k_B$, which gives $z_{nl}(k_{max}) \simeq 7$. Choosing $k_{max} \simeq 2\pi/0.8$ Mpc, then $k_B \simeq 2\pi/80$ kpc and all the observational constraints are satisfied, with $\langle B_0^2 \rangle^{1/2} \simeq 3 \times 10^{-9}$ G and $\bar{B}(l_g, t_0) \simeq 10^{-10}$ G. On the other hand, if $k_{max} \simeq 10^{-2}k_B \simeq 2\pi/8$ Mpc, then $t_{nl}(k_{max}) \simeq t_0$ and $k_B = 2\pi/0.08$ Mpc, which satisfies equation (10) but violates equation (49).

We see that with a more realistic choice of power spectra for magnetic fields at recombination, nonlinear structures in a cosmologically relevant range of scales can be formed at reasonable redshifts for field strengths below the observational upper limits. Although the number of parameters in this discussion is large, the physically relevant range is quite limited. As we improve our understanding of the evolution of magnetic fields from the early universe up to the epoch of galaxy formation, the parameter space will become more constrained. For instance, in the absence of primordial vorticity, magnetic field perturbations are damped up to the Silk damping scale and $k_{max} \lesssim 2\pi/10$ Mpc (Jedamzik et al. 1996).

5. CONCLUSIONS

We have studied the effects of magnetic fields present at recombination on the origin and evolution of density perturbations and peculiar velocities. We find that there are generic features of the generated density perturbations which are largely independent of the assumed spectrum of the primordial magnetic field. The first conclusion we can draw is that, within our linear perturbation approach, magnetic fields cannot explain the observed galaxy power spectrum on large scales, since the generated spectrum is too steep for small k. To produce the observed $P \propto k$ spectrum on large scales, we need $\tilde{b}^2(k) \propto k^{-3}$ for small k, with amplitudes that violate the observational constraints on $\langle B_0^2 \rangle$.

Another generic feature is the cutoff introduced by the magnetic Jeans length. This cutoff limits the amplitude of the power spectrum for any choice of magnetic field strength. As the magnetic field strength increases, the amplitude for a given density perturbation mode rises, but, simultaneously, the magnetic Jeans cutoff moves to smaller k. The net effect is that the peak amplitude for the resulting density power spectrum does not necessarily increase as one increases $\langle B_0^2 \rangle$.

Since the generated spectrum falls sharply at small k and is cut off at large k, magnetic fields generally produce a peak in the density spectrum over a narrow range of wavenumbers. For this peak to be of relevance to the formation of structure, the amplitude $\Delta(k, t_0)$ must be $\gtrsim 1$ for scales $2\pi k^{-1} \lesssim 8$ Mpc. The peak amplitude is sensitive to the assumed spectrum for the primordial magnetic field; the smaller the $k_{\max}$, the stronger the variance in the density perturbations. In particular, if $k_{\max} \lesssim k_B$, density variances well above unity can be obtained with relatively small magnetic fields. Depending on k_B and $k_{\max}$, objects from galaxy scales down to a first generation of massive stars can be formed. As the variance reaches unity, our calculations break down, and another conclusion can be drawn: when magnetic fields are important, their effects are mostly nonlinear in nature. Our linear calculations can, however, be used to estimate the epoch of nonlinear collapse of different mass scales.

In the present work, we have focused on a purely baryonic universe. In a subsequent paper, we study the evolution of density perturbations when nonbaryonic dark matter is the dominant component of the universe. When we include nonrelativistic (cold) dark matter, we find that the amplitude of the density perturbations decreases as $\Omega_{\rm baryon}$ decreases for a fixed magnetic field strength. On the other hand, the perturbations become unstable for all wavenumbers: since cold dark matter does not couple to the magnetic fields, no damped oscillatory modes can be sustained. In this case, the perturbation amplitude $\Delta(k)$ flattens out for large k rather than being cutoff at k_B. Baryons will still show some resistance to clumping on small scales due to the magnetic field; this may segregate baryons from dark matter, introducing a source of bias on small scales.

In the case of hot dark matter, the growth of baryon perturbations on small scales is slower due to neutrino free-streaming. Therefore, the initial perturbations need to be much larger for the final variance to be greater than 1. Clearly, the hot dark matter scenario would greatly benefit from a peak in the variance at large k so that structures can form on scales smaller than the neutrino free-streaming length and populate the problematic empty voids.

Finally, we conclude by noting that magnetic fields most likely play a dynamical role in the formation of galaxies and clusters of galaxies even if the original perturbations were caused by other sources.

We thank J. Frieman, A. Stebbins, S. I. Vainshtein, and I. Wasserman for useful discussions. This work was supported in part by a NASA Astrophysics Theory grant to the University of Chicago and NASA grant NAG 5-2788 at Fermilab.

APPENDIX A

In this Appendix, we derive equation (34), apply it to the two *Ansätze* for $\tilde{\boldsymbol{B}}(\boldsymbol{k})$, and derive equations (36) and (45). We begin with equation (31),

$$\nabla \cdot \dot{\boldsymbol{v}}(\boldsymbol{x}, t_{\rm rec}) = \alpha \nabla \cdot [(\nabla \times \boldsymbol{B}_0) \times \boldsymbol{B}_0] \,, \tag{A1}$$

where $\alpha \equiv \frac{1}{4}\pi \rho_0 R_{\rm rec}^2$. By using the Fourier expressions for $\boldsymbol{v}$ and $\boldsymbol{B}_0$, we obtain

$$i\boldsymbol{k} \cdot \dot{\tilde{\boldsymbol{v}}}(\boldsymbol{k}, t_{\rm rec}) = \alpha \int d^3\boldsymbol{k}_1 \, \boldsymbol{k} \cdot \{\boldsymbol{k}_1[\boldsymbol{B}(\boldsymbol{k}_1) \cdot \boldsymbol{B}(\boldsymbol{k} - \boldsymbol{k}_1)] - \boldsymbol{B}(\boldsymbol{k}_1)[\boldsymbol{k}_1 \cdot \boldsymbol{B}(\boldsymbol{k} - \boldsymbol{k}_1)]\} \,, \tag{A2}$$

where $\boldsymbol{B} \equiv \tilde{\boldsymbol{B}}$ throughout this Appendix. If we choose our coordinate system in such a way that $\boldsymbol{k}$ is along the z-axis,

$$\int d^3\boldsymbol{k}_1 = 4\pi \int dk_1 \, k_1^2 \int d\mu \,,$$

where $\mu \equiv \cos\theta$ with θ the angle between $\boldsymbol{k}_1$ and the z-axis. The integration range in equation (A2) should be taken carefully, since the integrand had $\delta(\boldsymbol{k} - \boldsymbol{k}_1 - \boldsymbol{k}_2)$ before the integrated over $\boldsymbol{k}_2$ with the condition of $k_{\min} \le k_i \le k_{\max}$ for $i = 1, 2$. In other words, there is a constraint on the angle to be integrated over, depending on the magnitude of k_1. By taking this constraint into account, the integration range of equation (A2) depends on the magnitude of k and can be shown as follows:

1. For $0 \le k \le k_{\min}$,

$$\int dk_1 \, d\mu = \int_{k_{\min}}^{k+k_{\min}} dk_1 \int_{-1}^{(k^2+k_1^2-k_{\min}^2)/2kk_1} d\mu + \int_{k+k_{\min}}^{k_{\max}-k} dk_1 \int_{-1}^{1} d\mu + \int_{k_{\max}-k}^{k_{\max}} dk_1 \int_{(k^2+k_1^2-k_{\max}^2)/2kk_1}^{1} d\mu \,. \tag{A3}$$

2. For $k_{\min} < k < k_{\max}$,

$$\int dk_1 \, d\mu = \int_{k_{\min}}^{k-k_{\min}} dk_1 \int_{-1}^{1} d\mu + \int_{k-k_{\min}}^{k+k_{\min}} dk_1 \int_{-1}^{(k^2+k_1^2-k_{\min}^2)/2kk_1} d\mu + \int_{k+k_{\min}}^{k_{\max}-k} dk_1 \int_{-1}^{1} d\mu + \int_{k_{\max}-k}^{k_{\max}} dk_1 \int_{(k^2+k_1^2-k_{\max}^2)/2kk_1}^{1} d\mu \,. \tag{A4}$$

3. For $k_{\max} \le k \le k_{\max} - k_{\min}$,

$$\int dk_1\, d\mu = \int_{k_{\min}}^{k-k_{\min}} dk_1 \int_{(k^2+k_1{}^2-k_{\max}{}^2)/2kk_1} d\mu + \int_{k-k_{\min}}^{k_{\max}} dk_1 \int_{(k^2+k_1{}^2-k_{\max}{}^2)/2kk_1}^{(k^2+k_1{}^2-k_{\min}{}^2)/2kk_1} d\mu\,. \tag{A5}$$

4. For $k_{\max} + k_{\min} \le k \le 2k_{\max}$,

$$\int dk_1\, d\mu = \int_{k_{\min}}^{k_{\max}} dk_1 \int_{(k^2+k_1{}^2-k_{\max}{}^2)/2kk_1} d\mu\,. \tag{A6}$$

If we take the ensemble average of both sides of equation (A2), and use equation (29), we obtain

$$\langle \boldsymbol{k}\cdot\dot{\tilde{\boldsymbol{v}}}(\boldsymbol{k}, t_{\rm rec})\rangle = 0\,.$$

To calculate $\dot{\tilde{v}}_{\rm rms}(k, t_{\rm rec})$, we take the square of both sides of equation (A2) and obtain

$$|\boldsymbol{k}\cdot\dot{\tilde{\boldsymbol{v}}}(\boldsymbol{k}, t_{\rm rec})|^2 = \alpha^2 \int d^3k_1\, d^3k_2 \{[-\boldsymbol{k}\cdot\boldsymbol{B}^*(\boldsymbol{k}_1)][\boldsymbol{k}_1\cdot\boldsymbol{B}^*(\boldsymbol{k}-\boldsymbol{k}_1)] + (\boldsymbol{k}\cdot\boldsymbol{k}_1)[\boldsymbol{B}^*(\boldsymbol{k}_1)\cdot\boldsymbol{B}^*(\boldsymbol{k}-\boldsymbol{k}_1)]\}$$
$$\times \{[-\boldsymbol{k}\cdot\boldsymbol{B}(\boldsymbol{k}_2)][\boldsymbol{k}_2\cdot\boldsymbol{B}(\boldsymbol{k}-\boldsymbol{k}_2)] + (\boldsymbol{k}\cdot\boldsymbol{k}_2)[\boldsymbol{B}(\boldsymbol{k}_2)\cdot\boldsymbol{B}(\boldsymbol{k}-\boldsymbol{k}_2)]\}\,. \tag{A7}$$

Then we take the ensemble average of both sides of equation (A7) and express the fourth-order correlation of B as a sum of a product of second-order correlations by assuming a Gaussian statistics for B. Since each fourth-order correlation gives three products of second-order ones, we obtain a total of 12 terms on the right-hand side of equation (A7). Applying equation (29) to these 12 terms yields terms proportional to $\delta(\boldsymbol{k})$, $\delta(\boldsymbol{k}_1-\boldsymbol{k}_2)$, and $\delta(\boldsymbol{k}-\boldsymbol{k}_1-\boldsymbol{k}_2)$, respectively. Four of these terms [which contain $\delta(\boldsymbol{k})$] vanish upon integration, and they will not be written here; retaining the remaining eight terms leads to the expression

$$\begin{aligned}\langle|\boldsymbol{k}\cdot\dot{\tilde{\boldsymbol{v}}}(\boldsymbol{k}, t_{\rm rec})|^2\rangle = \alpha^2 \int d^3k_1\, d^3k_2 [&\langle \boldsymbol{k}\cdot\boldsymbol{B}^*(\boldsymbol{k}_1)\boldsymbol{k}\cdot\boldsymbol{B}(\boldsymbol{k}_2)\rangle\langle \boldsymbol{k}_1\cdot\boldsymbol{B}^*(\boldsymbol{k}-\boldsymbol{k}_1)\boldsymbol{k}_2\cdot\boldsymbol{B}(\boldsymbol{k}-\boldsymbol{k}_2)\rangle\\
&+(\boldsymbol{k}\cdot\boldsymbol{k}_1)(\boldsymbol{k}\cdot\boldsymbol{k}_2)\langle B_i^*(\boldsymbol{k}_1)B_j(\boldsymbol{k}_2)\rangle\langle B_i^*(\boldsymbol{k}-\boldsymbol{k}_1)B_j(\boldsymbol{k}-\boldsymbol{k}_2)\rangle\\
&-(\boldsymbol{k}\cdot\boldsymbol{k}_2)\langle \boldsymbol{k}\cdot\boldsymbol{B}^*(\boldsymbol{k}_1)B_i(\boldsymbol{k}_2)\rangle\langle \boldsymbol{k}_1\cdot\boldsymbol{B}^*(\boldsymbol{k}-\boldsymbol{k}_1)B_i(\boldsymbol{k}-\boldsymbol{k}_2)\rangle\\
&-(\boldsymbol{k}\cdot\boldsymbol{k}_1)\langle \boldsymbol{k}\cdot\boldsymbol{B}(\boldsymbol{k}_2)B_i^*(\boldsymbol{k}_1)\rangle\langle \boldsymbol{k}_2\cdot\boldsymbol{B}(\boldsymbol{k}-\boldsymbol{k}_2)B_i^*(\boldsymbol{k}-\boldsymbol{k}_1)\rangle\\
&+\langle \boldsymbol{k}\cdot\boldsymbol{B}^*(\boldsymbol{k}_1)\boldsymbol{k}_2\cdot\boldsymbol{B}(\boldsymbol{k}-\boldsymbol{k}_2)\rangle\langle \boldsymbol{k}\cdot\boldsymbol{B}(\boldsymbol{k}_2)\boldsymbol{k}_1\cdot\boldsymbol{B}^*(\boldsymbol{k}-\boldsymbol{k}_1)\rangle\\
&+(\boldsymbol{k}\cdot\boldsymbol{k}_1)(\boldsymbol{k}\cdot\boldsymbol{k}_2)\langle B_i^*(\boldsymbol{k}_1)B_j(\boldsymbol{k}-\boldsymbol{k}_2)\rangle\langle B_i^*(\boldsymbol{k}-\boldsymbol{k}_1)B_j(\boldsymbol{k}_2)\rangle\\
&-(\boldsymbol{k}\cdot\boldsymbol{k}_2)\langle \boldsymbol{k}\cdot\boldsymbol{B}^*(\boldsymbol{k}_1)B_i(\boldsymbol{k}-\boldsymbol{k}_2)\rangle\langle \boldsymbol{k}_1\cdot\boldsymbol{B}^*(\boldsymbol{k}-\boldsymbol{k}_1)B_i(\boldsymbol{k}_2)\rangle\\
&-(\boldsymbol{k}\cdot\boldsymbol{k}_1)\langle \boldsymbol{k}\cdot\boldsymbol{B}(\boldsymbol{k}_2)B_i^*(\boldsymbol{k}-\boldsymbol{k}_1)\rangle\langle \boldsymbol{k}_2\cdot\boldsymbol{B}(\boldsymbol{k}-\boldsymbol{k}_2)B_i^*(\boldsymbol{k}_1)\rangle]\\
\equiv k^2\dot{\tilde{v}}_{\parallel\,\rm rms}^2(\boldsymbol{k}, t_{\rm rec})\,,&\end{aligned} \tag{A8}$$

where $\boldsymbol{k}\cdot\dot{\tilde{\boldsymbol{v}}}(\boldsymbol{k}, t_{\rm rec}) \equiv k\dot{\tilde{v}}_{\parallel}(\boldsymbol{k}, t_{\rm rec})$. The integral of these eight terms is given by (using eq. [29]),

$$k^2\dot{\tilde{v}}_{\parallel\,\rm rms}^2(k, t_{\rm rec}) = \frac{\alpha^2 V k^2}{(4\pi)^2}\int_{k_{\min}}^{k_{\max}} dk_1\, k_1^2 \int_{-1}^{1} d\mu\, \frac{B^2(k_1)B^2(|\boldsymbol{k}-\boldsymbol{k}_1|)}{|\boldsymbol{k}-\boldsymbol{k}_1|^2}\,[2k^3k_1\,\mu + k^2k_1^2(1-5\mu^2) + 2kk_1^3\,\mu^3]\,, \tag{A9}$$

where the identity $\delta(\boldsymbol{k}=0) = V/(2\pi)^3$ has been used. Equations (A8) and (A9) give equation (34).

For the delta function *Ansätz*, $B^2(k) = \langle B_0^2\rangle\delta(k-k_*)/4\pi k^2$, and therefore

$$k^2\dot{\tilde{v}}_{\parallel\,\rm rms}^2(k, t_{\rm rec}) = \frac{\alpha^2 V\langle B_0^2\rangle^2}{(4\pi)^4}\frac{k^3}{k_*^2}\,. \tag{A10}$$

Equation (36) follows from this result.

Now we evaluate $\dot{\tilde{v}}_{\parallel\,\rm rms}^2$ for the case of a power-law spectrum for $\tilde{B}^2(k)$, as in equation (44). For simplicity, we assume $k_{\min} = 0$. The resulting integral can be solved analytically if we use $k/k_{\max}$ as a small parameter. In such an expansion, the leading-order term turns out to be $(k/k_{\max})^3$ for $q = -2$, and $(k/k_{\max})^4$ for $q = -1$, 0, 1, 2, 3, 4, and 6. Finally, we find the following solution for the $q \ge -1$ case:

$$k^2\dot{\tilde{v}}_{\parallel\,\rm rms}^2(k, t_{\rm rec}) = \frac{\alpha^2 V}{(4\pi)^4}\,A^2k_{\max}^{2q+3}k^4\,\frac{22}{15(2q+3)}\left[1 + O\left(\frac{k}{k_{\max}}\right)\right]. \tag{A11}$$

Therefore,

$$\langle|\boldsymbol{k}\cdot\dot{\tilde{\boldsymbol{v}}}(\boldsymbol{k}, t_{\rm rec})|^2\rangle = k^2\dot{\tilde{v}}_{\parallel\,\rm rms}^2(k, t_{\rm rec}) \simeq \frac{\alpha^2 V}{(4\pi)^4}\langle B_0^2\rangle^2\frac{k^4}{k_{\max}^3}\frac{22(q+3)}{15(2q+3)}\,, \tag{A12}$$

where we used $\langle B_0^2\rangle = 4\pi\int_{k_{\min}}^{k_{\max}} dk k^2 Ak^q \simeq Ak_{\max}^{q+3}/(q+3)$; this leads directly to equation (45).

APPENDIX B

In this Appendix, we demonstrate that $\langle B_{\rm rec}\tilde{v}_{\parallel}(t)\rangle = \langle B_{\rm rec}\tilde{v}_{\perp}(t)\rangle = 0$. We begin with the evolution equation for $\tilde{v}_{\parallel}$, obtained through equation (54):

$$k(t^2\partial_{tt} + 2t\partial_t - \tfrac{4}{9})\tilde{v}_{\parallel}(\boldsymbol{k}, t) = \beta \int d^3\boldsymbol{k}_1\, d^3\boldsymbol{k}_2\, F[\boldsymbol{k}, \boldsymbol{k}_1, \boldsymbol{k}_2, \tilde{\boldsymbol{B}}(\boldsymbol{k}_1), \tilde{\boldsymbol{B}}(\boldsymbol{k}_2), \tilde{\boldsymbol{v}}(\boldsymbol{k} - \boldsymbol{k}_1 - \boldsymbol{k}_2, t)] \,. \tag{B1}$$

With the use of Green's function for this equation,

$$G(t, t') = \frac{3\theta(t - t')}{5kt'}\left[\left(\frac{t'}{t}\right)^{-1/3} - \left(\frac{t'}{t}\right)^{4/3}\right] \tag{B2}$$

(where θ is the step function), one can solve equation (B1) formally, given the initial conditions

$$\tilde{v}_{\parallel}(k, t_{\rm rec}) = 0$$

and

$$\partial_t \tilde{v}_{\parallel}(k, t)\,|_{t=t_{\rm rec}} = \dot{\tilde{v}}_{\parallel}(k, t_{\rm rec}) \,.$$

This Green's function solution is given by

$$\tilde{v}_{\parallel}(k, t) = \frac{3t_{\rm rec}\,\dot{\tilde{v}}_{\parallel}(k, t_{\rm rec})}{5}\left[\left(\frac{t_{\rm rec}}{t}\right)^{-1/3} - \left(\frac{t_{\rm rec}}{t}\right)^{4/3}\right]$$
$$+ \beta \int_{t_{\rm rec}}^{t} dt' \int d^3\boldsymbol{k}_1\, d^3\boldsymbol{k}_2\, G(t, t')F[\boldsymbol{k}, \boldsymbol{k}_1, \boldsymbol{k}_2, \tilde{\boldsymbol{B}}(\boldsymbol{k}_1), \tilde{\boldsymbol{B}}(\boldsymbol{k}_2), \tilde{\boldsymbol{v}}(\boldsymbol{k} - \boldsymbol{k}_1 - \boldsymbol{k}_2, t')] \,. \tag{B3}$$

This equation can be solved by iteration, yielding a Born series solution, for which the zeroth-order iterate $\tilde{v}^0_{\parallel}(k, t)$ is given by

$$\tilde{v}^0_{\parallel}(k, t) = \frac{3t_{\rm rec}\,\dot{\tilde{v}}_{\parallel}(k, t_{\rm rec})}{5}\left[\left(\frac{t_{\rm rec}}{t}\right)^{-1/3} - \left(\frac{t_{\rm rec}}{t}\right)^{4/3}\right]. \tag{B4}$$

We note first that $\langle\tilde{v}^0_{\parallel}(k, t)B_{\rm rec}\rangle = 0$. This result is obtained simply by noting that $\dot{\tilde{v}}^0_{\parallel}(k, t_{\rm rec})$ is quadratic in $B_{\rm rec}$ (see eq. [55]), so that $\tilde{v}^0_{\parallel}(k, t)B_{\rm rec}$ is an odd product of $B_{\rm rec}$. Hence, as long as $B_{\rm rec}$ is a random variable governed by Gaussian statistics, $\langle\tilde{v}^0_{\parallel}(k, t)B_{\rm rec}\rangle$ must vanish, since all odd moments of a Gaussian random variable vanish.

It is now straightforward to demonstrate that $\langle\tilde{v}_{\parallel}(k, t)B_{\rm rec}\rangle = 0$ to all orders by simply computing the next-order iterates: At the nth iteration stage, $\tilde{v}^n_{\parallel}(k, t)$ is the sum of even products of $B_{\rm rec}$ (because F is a quadratic form in $B_{\rm rec}$); hence, $\tilde{v}^n_{\parallel}(k, t)B_{\rm rec}$ must be always an odd product of $B_{\rm rec}$, and therefore $\langle\tilde{v}^n_{\parallel}(k, t)B_{\rm rec}\rangle = 0$, as before. Thus, under the assumption that the Born series expansion converges, we obtain a portion of our desired result, namely that

$$\langle\tilde{v}_{\parallel}(k, t)B_{\rm rec}\rangle = 0 \,.$$

It is now readily shown that the same result obtains for the incompressible flow, $\tilde{v}_{\perp}$, by simply repeating the above calculation, but now projecting out the incompressible component. Thus, we also obtain $\langle\tilde{v}_{\perp}(k, t)B_{\rm rec}\rangle = 0$, and hence we have the ultimately desired result that

$$\langle\tilde{v}(k, t)B_{\rm rec}\rangle = 0 \,.$$

APPENDIX C

In this Appendix, we show how to obtain $\tilde{\delta}_{\rm rms}(k, t)$ from $\tilde{v}_{\rm rms}(k, t)$ in the force-free case of § 4. We start with equation (55) in the main text, which reads

$$\left(\partial_{TT} + \partial_T - \frac{4}{9}\right)\tilde{v}_{\parallel}(\boldsymbol{k}, T) = \frac{\beta}{k}\, G_i(\boldsymbol{k}:\boldsymbol{l})\tilde{v}_i(\boldsymbol{l}, T) \,. \tag{C1}$$

Upon using $T \equiv \ln t$, this is equivalent to

$$\left(t^2\partial_{tt} + 2t\partial_t - \frac{4}{9}\right)\tilde{v}_{\parallel}(\boldsymbol{k}, t) = \frac{\beta}{k}\, G_i(\boldsymbol{k}:\boldsymbol{l})\tilde{v}_i(\boldsymbol{l}, t) \,. \tag{C2}$$

The rms solution to equation (C2) was shown to be given by equation (58) in the main text, which we rewrite as

$$\tilde{v}_{\parallel,\,\rm rms}(k, t) = \dot{\tilde{v}}_{\parallel,\,\rm rms}(k, t_{\rm rec})V(t) \,, \tag{C3}$$

where

$$V(t) \equiv \frac{3t_{\rm rec}}{m}\left(\frac{t}{t_{\rm rec}}\right)^{-1/2}\left[\left(\frac{t}{t_{\rm rec}}\right)^{m/6} - \left(\frac{t}{t_{\rm rec}}\right)^{-m/6}\right],$$

$\tilde{v}_{\rm rms}(k, t) \equiv (<|\tilde{v}_{\parallel}(\boldsymbol{k}, t)|^2>)^{1/2}$, and $m \equiv (25 - 12ak^2)^{1/2}$.

First, we multiply both sides of equation (C2) by $\tilde{v}^*_{\parallel}(\boldsymbol{k}, t')$, with $t' \neq t$, and then we take an average to get the following equation:

$$\left(t^2\partial_{tt} + 2t\partial_t - \frac{4}{9}\right)\langle\tilde{v}_{\parallel}(\boldsymbol{k}, t)\tilde{v}^*_{\parallel}(\boldsymbol{k}, t')\rangle = \frac{\beta}{k}\langle G_i(\boldsymbol{k}:\boldsymbol{l})v_i(\boldsymbol{l}, t)\tilde{v}^*_{\parallel}(\boldsymbol{k}, t')\rangle . \tag{C4}$$

Now repeating the same calculation that was used to obtain equation (57) from equation (56), it can be shown that

$$\langle G_i(\boldsymbol{k}:\boldsymbol{l})\tilde{v}_i(\boldsymbol{l}, t)\tilde{v}^*_{\parallel}(\boldsymbol{k}, t')\rangle = -\tfrac{2}{3}\langle B_0^2\rangle k^3\langle\tilde{v}_{\parallel}(\boldsymbol{k}, t)\tilde{v}^*_{\parallel}(\boldsymbol{k}, t')\rangle . \tag{C5}$$

Using equation (C5), we readily obtain the solution to equation (C4), namely

$$<\tilde{v}_{\parallel}(\boldsymbol{k}, t)\tilde{v}^*_{\parallel}(\boldsymbol{k}, t')> = \langle\dot{\tilde{v}}_{\parallel}(\boldsymbol{k}, t_{\rm rec})\tilde{v}^*_{\parallel}(\boldsymbol{k}, t')\rangle V(t) . \tag{C6}$$

Next, let us take the complex conjugate of both sides of equation (C2), multiply by $\dot{\tilde{v}}_{\parallel}(\boldsymbol{k}, t_{\rm rec})$, and then take an average; that gives

$$\langle\tilde{v}^*_{\parallel}(\boldsymbol{k}, t)\dot{\tilde{v}}_{\parallel}(\boldsymbol{k}, t_{\rm rec})\rangle = \langle|\dot{\tilde{v}}_{\parallel}(\boldsymbol{k}, t_{\rm rec})|^2\rangle V(t) . \tag{C7}$$

From equations (C3) and (C7),

$$\tilde{v}^*_{\parallel}(\boldsymbol{k}, t)\dot{\tilde{v}}_{\parallel}(\boldsymbol{k}, t_{\rm rec})\rangle = \sqrt{\langle|\dot{\tilde{v}}_{\parallel}(\boldsymbol{k}, t_{\rm rec})|^2\rangle}\sqrt{\langle|\tilde{v}_{\parallel}(\boldsymbol{k}, t)|^2\rangle} ,$$

or

$$\tilde{v}^*_{\parallel}(\boldsymbol{k}, t')\dot{\tilde{v}}_{\parallel}(\boldsymbol{k}, t_{\rm rec})\rangle = \sqrt{\langle|\dot{\tilde{v}}_{\parallel}(\boldsymbol{k}, t_{\rm rec})|^2\rangle}\sqrt{\langle|\tilde{v}_{\parallel}(\boldsymbol{k}, t')|^2\rangle} . \tag{C8}$$

Upon using equation (C8) in equation (C6),

$$\tilde{v}_{\parallel}(\boldsymbol{k}, t)\tilde{v}^*_{\parallel}(\boldsymbol{k}, t')\rangle = \sqrt{\langle|\dot{\tilde{v}}_{\parallel}(\boldsymbol{k}, t_{\rm rec})|^2\rangle}\sqrt{\langle|\tilde{v}_{\parallel}(\boldsymbol{k}, t')|^2\rangle}V(t) . \tag{C9}$$

Finally, with the help of equation (C3), equation (C9) becomes

$$\tilde{v}_{\parallel}(\boldsymbol{k}, t)\tilde{v}^*_{\parallel}(\boldsymbol{k}, t')\rangle = \sqrt{\langle|\tilde{v}_{\parallel}(\boldsymbol{k}, t)|^2\rangle}\sqrt{\langle|\tilde{v}_{\parallel}(\boldsymbol{k}, t')|^2\rangle} . \tag{C10}$$

On the other hand, equation (12) in the main text gives us the following equation:

$$ik\frac{\tilde{v}_{\parallel}(\boldsymbol{k}, t)}{R(t)} = -\frac{\partial}{\partial t}\tilde{\delta}(\boldsymbol{k}, t) . \tag{C11}$$

By integrating equation (C11), the solution for the density fluctuations is

$$\tilde{\delta}(\boldsymbol{k}, t) = -ik\int_{t_{\rm rec}}^{t} dt'\,\frac{\tilde{v}_{\parallel}(\boldsymbol{k}, t')}{R(t')} . \tag{C12}$$

By multiplying by the complex conjugate of equation (C12), and then taking its average, we obtain

$$\begin{aligned}\langle|\tilde{\delta}(\boldsymbol{k}, t)|^2\rangle &= k^2\int_{t_{\rm rec}}^{t}\frac{dt_1}{R(t_1)}\int_{t_{\rm rec}}^{t}\frac{dt_2}{R(t_2)}\langle\tilde{v}_{\parallel}(\boldsymbol{k}, t_1)\tilde{v}^*_{\parallel}(\boldsymbol{k}, t_2)\rangle \\ &= k^2\int_{t_{\rm rec}}^{t}\frac{dt_1}{R(t_1)}\sqrt{\langle|\tilde{v}_{\parallel}(\boldsymbol{k}, t_1)|^2\rangle}\int_{t_{\rm rec}}^{t}\frac{dt_2}{R(t_2)}\sqrt{\langle|\tilde{v}_{\parallel}(\boldsymbol{k}, t_2)|^2\rangle} \\ &= \left[k\int_{t_{\rm rec}}^{t}\frac{dt_1}{R(t_1)}\sqrt{\langle|\tilde{v}_{\parallel}(\boldsymbol{k}, t_1)|^2\rangle}\right]^2 ,\end{aligned} \tag{C13}$$

where equation (C10) has been used; taking the square root of equation (C13), we obtain

$$\sqrt{\langle|\tilde{\delta}(\boldsymbol{k}, t)|^2\rangle} = k\int_{t_{\rm rec}}^{t}\frac{dt_1}{R(t_1)}\sqrt{\langle|\tilde{v}_{\parallel}(\boldsymbol{k}, t_1)|^2\rangle} . \tag{C14}$$

In other words,

$$\tilde{\delta}_{\rm rms}(k, t) = k\int_{t_{\rm rec}}^{t}\frac{dt_1}{R(t_1)}\tilde{v}_{\rm rms}(k, t_1) . \tag{C15}$$

The differential equation for $\tilde{\delta}_{\rm rms}$ follows via taking the time derivative of equation (C15),

$$\frac{\partial}{\partial t}\,\tilde{\delta}_{\rm rms}(k,\,t) = k\,\frac{\tilde{v}_{\rm rms}(k,\,t)}{R(t)}\,. \tag{C16}$$

APPENDIX D

In this Appendix, we show how to derive equations (69) and (74). We begin with equation (65),

$$\nabla\cdot\dot{\boldsymbol{v}}(\boldsymbol{x},\,t_{\rm rec}) = \alpha\{\nabla\cdot[(\nabla\times\boldsymbol{B}_{\rm ff0})\times\boldsymbol{b}_0] + \nabla\cdot[(\nabla\times\boldsymbol{b}_0)\times\boldsymbol{B}_{\rm ff0}]\}\,, \tag{D1}$$

where, again, $\alpha \equiv \frac{1}{4}\pi\rho_0 R_{\rm rec}^2$. By using the Fourier expressions for $\boldsymbol{v}$, $\boldsymbol{B}_{\rm ff0}$, and $\boldsymbol{b}_0$, we obtain

$$i\boldsymbol{k}\cdot\dot{\tilde{\boldsymbol{v}}}(\boldsymbol{k},\,t_{\rm rec}) = \alpha\int d^3\boldsymbol{k}_1\{k^2[\tilde{\boldsymbol{b}}(\boldsymbol{k}_1)\cdot\tilde{\boldsymbol{B}}_{\rm ff}(\boldsymbol{k}-\boldsymbol{k}_1)] - [(\boldsymbol{k}+\boldsymbol{k}_1)\cdot\tilde{\boldsymbol{B}}_{\rm ff}(\boldsymbol{k}-\boldsymbol{k}_1)][\boldsymbol{k}\cdot\tilde{\boldsymbol{b}}(\boldsymbol{k}_1)]\}\,, \tag{D2}$$

where $\tilde{\boldsymbol{B}}_{\rm ff}(\boldsymbol{k})$ is the Fourier transform of $\boldsymbol{B}_{\rm ff0}$, and $\tilde{\boldsymbol{b}}(\boldsymbol{k})$ is the transform of $\boldsymbol{b}_0$. The ensemble averages of both sides of equation (D2) vanish. Again, we compute $\tilde{v}_{\rm rms}(k,\,t_{\rm rec})$ by taking the square of both sides of equation (D2) and then ensemble average, with the following result:

$$\langle|\boldsymbol{k}\cdot\dot{\tilde{\boldsymbol{v}}}(\boldsymbol{k},\,t_{\rm rec})|^2\rangle = \alpha^2\,\frac{Vk^2}{2\pi^2}\int_{k_{\rm min}}^{k_{\rm max}} dk_1\,k_1^2\int_{-1}^{1} d\mu\,\frac{\tilde{b}^2(k_1)\tilde{B}_{\rm ff}^2(|\boldsymbol{k}-\boldsymbol{k}_1|)}{|\boldsymbol{k}-\boldsymbol{k}_1|^2}\,[k^4 + k^2k_1^2(1-\mu^2+\mu^4) - k^3k_1\,\mu(1+\mu^2)]\,. \tag{D3}$$

The polynomial integrand in equation (D3) is not the same as in equation (A9), since $\boldsymbol{B}_{\rm ff}$ and b are assumed to be uncorrelated and separated in k-space (scale separation). This assumption changes the nontrivial contributions in equation (A8).

For the force-free background magnetic field, we assume a delta function spectrum and write

$$\tilde{B}_{\rm ff}^2(k) \equiv \langle B_{\rm ff0}^2\rangle\,\frac{\delta(k-k_0)}{4\pi k^2}\,, \tag{D4}$$

where we assume that k_0 is small compared to the wavenumber of the fluctuations about the force-free background. Equation (D3) now takes the form

$$\begin{aligned}\langle|\boldsymbol{k}\cdot\dot{\tilde{\boldsymbol{v}}}(k,\,t_{\rm rec})|^2\rangle = {}& \frac{\alpha^2\langle B_{\rm ff0}^2\rangle V}{4(4\pi)^3kk_0^3}\int_{k_{\rm min}}^{k_{\rm max}} dk_1\,\frac{\tilde{b}^2(k_1)}{k_1}\,[k_1^8 - (4k_0^2+2k^2)k_1^6 + (6k_0^4+2k^2k_0^2)k_1^4 \\ & + (-4k_0^6 + 2k^2k_0^4 + 16k^4k_0^2 + 2k^6)k_1^2 + k_0^8 - 2k^2k_0^6 + 2k^6k_0^2 - k^8]\,.\end{aligned} \tag{D5}$$

For a delta function *Ansätz* for $\tilde{b}^2(k)$,

$$\tilde{b}^2(k) = \langle b_0^2\rangle\,\frac{\delta(k-k_b)}{4\pi k^2}\,,$$

only modes satisfying $k_b - k_0 \le k \le k_b + k_0$ are excited. With the use of equation (D5), the spectrum of the generated compressible modes is given by

$$k^2\dot{\tilde{v}}_{\parallel\,\rm rms}^2(k,\,t_{\rm rec}) \simeq \frac{4\alpha^2Vk^3}{(4\pi)^4k_bk_0}\,\langle B_{\rm ff0}^2\rangle\langle b_0^2\rangle F_\delta(k,\,k_0,\,k_b)\,, \tag{D6}$$

where

$$F_\delta(k,\,k_0,\,k_b) \equiv 1 + \frac{(k_b^2-k_0^2)^4 - 2k^2(k_b^2-k_0^2)(k_b^4-k_0^4) + 2k^6(k_b^2+k_0^2) - k^8}{16k^4k_b^2k_0^2}\,, \tag{D7}$$

from which equation (69) follows.

In the limit $k_b \to k_0$and for $k \ll 2k_b$, we recover the result in equation (A10) with an overall factor of 4 difference due to the relation between $\langle B_{\rm ff0}^2\rangle$, $\langle b_0^2\rangle$, and $\langle B_0^2\rangle$.

The power-law Ansätz cannot be written as

$$\tilde{b}^2(k_1) = Ck_1^q\,,$$

for $k_{\rm min} \le k_1 \le k_{\rm max}$, and $\langle b_0^2\rangle = 4\pi C\,(k_{\rm max}^{q+3} - k_{\rm min}^{q+3})/(q+3) \simeq 4\pi C\,k_{\rm max}^{q+3}/(q+3)$ for $k_{\rm min}$ and $k_{\rm max}$. Substituting this Ansätz in equation (D5), the integration can be performed within the following range: for $k \ge k_{\rm max} - k_0$, the upper limit on k_1 is $\max(k_1) = k_{\rm max}$, and for $k \le k_{\rm max} - k_0$, $\max(k_1) = k + k_0$; while for $k \le (k_0^2 + k_{\rm min}^2)^{1/2}$, the lower limit is $\min(k_1) = k_{\rm min}$, and finally, for $k \ge (k_0^2 + k_{\rm min}^2)^{1/2}$, $\min(k_1) = (k^2 - k_0^2)^{1/2}$. The solution for specific choices of k_0, $k_{\rm min}$, $k_{\rm max}$, and q is plotted in Figures 2 and 3.

Since $k_0 \ll k_{\rm min} \ll k_{\rm max}$, the most relevant range of the integration is $(k_0^2 + k_{\rm min}^2)^{1/2} \leq k \leq k_{\rm max} - k_0$. In this range, the integral in equation (D5) can be written as

$$k^2 \tilde{v}^2_{\parallel \rm rms}(k, t_{\rm rec}) \simeq \frac{\alpha^2 V}{4(4\pi)^4} \langle B^2_{\rm ff0} \rangle \langle b_0^2 \rangle \frac{k_{\rm max}^5}{k_0^3 k} (q+3) F_q(k, k_0, k_{\rm max}) , \tag{D8}$$

where

$$F_q(k, k_0, k_{\rm max}) \equiv \frac{1}{q+8} - \frac{4\kappa_0^2 + 2\kappa^2}{q+6} + \frac{6\kappa_0^4 + 2\kappa_0^2 \kappa^2}{q+4} + \frac{2\kappa^6 - 4\kappa_0^6 + 2\kappa^2 \kappa_0^4 + 16\kappa^4 \kappa_0^2}{q+2} + \frac{\kappa_0^8 - 2\kappa^2 \kappa_0^6 + 2\kappa^6 \kappa_0^2 - \kappa^8}{q} ; \tag{D9}$$

$\kappa_0 \equiv k_0/k_{\rm max}$ and $\kappa \equiv k/k_{\rm max}$. In the limit $\kappa_0 \ll \kappa$, $F_q \simeq 16 \kappa_0^3 \kappa^{q+5}$ and, therefore,

$$k^2 \tilde{v}^2_{\parallel \rm rms}(k, t_{\rm rec}) \simeq \frac{\alpha^2 V}{64\pi^4} \langle B^2_{\rm ff0} \rangle \langle b_0^2 \rangle (q+3) k \left(\frac{k}{k_{\rm max}} \right)^{q+3} . \tag{D10}$$

REFERENCES

Barrow, J. 1976, MNRAS, 175, 359
Cattaneo, F. 1994, ApJ, 434, 200
Cattaneo, F., & Vainshtein, S. I. 1991, ApJ, 376, L21
Chakrabarti, S. K., Rosner, R., & Vainshtein, S. 1994, Nature, 368, 434
Cheng, B., & Olinto, A. V. 1994, Phys. Rev. D, 50, 2421
Cheng, B., Schramm, D., & Truran, J. 1994, Phys. Rev. D, 49, 5006
Collins, C. A., Nichol, R. C., & Lumsden, S. L. 1992, MNRAS, 254, 295
Dolgov, A. D. 1993, Phys. Rev. D, 48, 2499
Dolgov, A. D., & Silk, J. 1993, Phys. Rev. D, 47, 3144
Efstathiou, G., et al. 1990, MNRAS, 247, 10P
Fisher, K. B., et al. 1993, ApJ, 402, 42
Ganga, K., Cheng, E., Meyer, S., & Page, L. 1993, ApJ, 410, L57
Geller, M., & Huchra, J. 1989, Science, 246, 897
Grasso, D., & Rubinstein, H. R. 1995, Astropart. Phys., 3, 95
Gruzinov, A. V., & Diamond, P. H. 1994, Phys. Rev. Lett., 72, 1651
Hogan, C. J. 1983, Phys. Rev. Lett., 51, 1488
Jedamzik, K., Katalinic, V., & Olinto, A. 1996, ApJ, submitted
Kernan, P., Starkman, G., & Vachaspati, T. 1995, CWRU-P10-95
Ko, C. M., & Parker, E. N. 1989, ApJ, 341 828
Kraichman, R. H., & Nagarajan, S. 1967, Phys. Fluids, 10, 859
Kronberg, P. P. 1994, Rep. Prog. Phys., 57, 325
Kronberg, P. P., & Perry, J. J. 1982, ApJ, 263, 518
Kronberg, P. P., Perry, J. J., & Zukowski, E. L. H. 1992, ApJ, 387, 528
Kronberg, P. P., & Simard-Normandin, M. 1976, Nature, 263, 653
Kulsrud, R. M. 1988, in Proc. Varenna Conf. Plasma Astrophys., ed. R. Gutenne (ESA SP-285), 531
———. 1995, private communication
Kulsrud, R. M., & Anderson, S. W. 1992, ApJ, 396, 606
Lee, S., Olinto, A., & Sigl, G. 1995, ApJ, 455, L21
Maddox, S. J., et al. 1990, MNRAS, 246, 433
Moffatt, H. K. 1978, Magnetic Field Generation in Electrically-Conducting Fluids (Cambridge: Cambridge Univ. Press)
Parker, E. N. 1979, Cosmical Magnetic Fields (Oxford: Oxford Univ. Press)
———. 1992, ApJ, 401, 137
Peebles, P. J. E. 1980, The Large-Scale Structure of The Universe (Princeton: Princeton Univ. Press)
———. 1993, Principles of Physical Cosmology (Princeton: Princeton Univ. Press)
Quashnock, J., Loeb, A., & Spergel, D. N. 1989, ApJ, 344, L49
Ratra, B. 1992a, ApJ, 391, L1
———. 1992b, Phys. Rev. D, 45, 1913
Rosner, R., & DeLuca, E. E. 1989, in The Center of the Galaxy, ed. M. Morris (Dordrecht: Kluwer), 319
Smoot, G., et al. 1992, ApJ, 396, L1
Taylor, J. B. 1974, Phys. Rev. Lett., 33, 1139
Turner, M. S., & Widrow, L. M. 1988, Phys. Rev. D, 30, 2743
Vainshtein, S. I., & Rosner, R. 1991, ApJ, 376, 199
Vaschaspati, T. 1991, Phys. Lett. B, 265, 258
Wasserman, I. 1978, ApJ, 224, 337
Wolfe, A. M. 1988, in QSO Absorption Lines: Probing the Universe, ed. C. J. Blades et al. (Cambridge: Cambridge Univ. Press), 297
Wolfe, A. M., Lanzetta, K. M., & Oren, A. L. 1991, ApJ, 388, 17
Woltjer, L. 1958, Proc. Natl. Acad. Sci., 44, 489
Zweibel, E. G. 1988, ApJ, 329, 384